Atmos. Chem. Phys. Discuss., 9, 19713–19781, 2009
www.atmos-chem-phys-discuss.net/9/19713/2009/

Atmospheric Chemistry and Physics Discussions

This discussion paper is/has been under review for the journal *Atmospheric Chemistry and Physics (ACP)*. Please refer to the corresponding final paper in *ACP* if available.

An overview of the SCOUT-AMMA stratospheric aircraft, balloons and sondes campaign in West Africa, August 2006: rationale, roadmap and highlights

F. Cairo[1], J. P. Pommereau[2], K. S. Law[2], H. Schlager[3], A. Garnier[2], F. Fierli[1], M. Ern[4], M. Streibel[5], S. Arabas[6], S. Borrmann[7,8], J. J. Berthelier[2], C. Blom[9], T. Christensen[10], F. D'Amato[11], G. Di Donfrancesco[12], T. Deshler[13], A. Diedhiou[14], G. Durry[15], O. Engelsen[16], F. Goutail[2], N. R. P. Harris[5], E. R. T. Kerstel[17], S. Khaykin[18], P. Konopka[4], A. Kylling[16], N. Larsen[10], T. Lebel[19], X. Liu[15], A. R. MacKenzie[20], J. Nielsen[10], A. Oulanowski[18], D. J. Parker[21], J. Pelon[2], J. Polcher[22], J. A. Pyle[23,30], F. Ravegnani[1], E. D. Rivière[15], A. D. Robinson[23], T. Röckmann[24], C. Schiller[4], F. Simões[2], L. Stefanutti[25,26], F. Stroh[4], L. Some[27], P. Siegmund[28], N. Sitnikov[18], J. P. Vernier[2], C. M. Volk[29], C. Voigt[3,7], M. von Hobe[4], S. Viciani[11], and V. Yushkov[18]

[1]Istituto di Scienze dell'Atmosfera e del Clima, Consiglio Nazionale delle Ricerche, Roma, Italy

[2]LATMOS, CNRS UMR-7620, St-Maur-des-Fosses, France
[3]DLR Institut für Physik der Atmosphäre, Oberpfaffenhofen, Germany
[4]ICG-1, Forschungszentrum Jülich, Jülich, Germany
[5]European Ozone Research Coordinating Unit, Cambridge University, Cambridge, UK
[6]Institute of Geophysics, University of Warsaw, Warsaw, Poland
[7]Institute of Atmospheric Physics, University of Mainz, Mainz, Germany
[8]Max-Planck Institute for Chemistry, Particle Chemistry Department, Mainz, Germany
[9]Institut für Meteorologie und Klimaforschung (IMK), Forschungszentrum Karlsruhe und Universität Karlsruhe, Karlsruhe, Germany
[10]Danish Meteorological Institute, Copenhagen, Denmark
[11]Istituto Nazionale di Ottica Applicata, Consiglio Nazionale delle Ricerche, Firenze, Italy
[12]Ente Nazionale per le Nuove tecnologie, l'Energia e l'Ambiente, Frascati, Italy
[13]Department of Atmospheric Sciences, Wyoming University, Laramie, USA
[14]Institut de Recherche pour le Developpement-NIGER, Niamey, Niger
[15]Groupe de Spectroscopie Moleculaire et Atmospherique, Faculté des Sciences, Université de Reims Champagne-Ardenne and CNRS, Reims, France
[16]Norwegian Institute for Air Research, Oslo, Norway
[17]Center for Isotope Research, University of Groningen, Groningen, The Netherlands
[18]Central Aerological Observatory, Moscow, Russian Federation
[19]LTHE (UMR 5564), Institut de Recherche pour le Developpement-FRANCE, Grenoble, France
[20]Lancaster Environmental Centre, Lancaster University, Lancaster, UK
[21]School of Earth and Environment, University of Leeds, Leeds, UK
[22]Laboratoire de Meteoreologie Dinamique, CNRS, Paris, France
[23]Chemistry Department, Cambridge University, Cambridge, UK
[24]Institute for Marine and Atmospheric Research Utrecht, Utrecht University, Utrecht, The Netherlands

ACPD
9, 19713–19781, 2009

[25]Istituto di Ricerche per la Protezione Idrogeologica, Consiglio Nazionale delle Ricerche, Firenze, Italy
[26]Geophysica-EEIG, Firenze, Italy
[27]INERA, Ouagadougou, Burkina Faso
[28]Royal Netherlands Meteorological Institute - KNMI, The Netherlands
[29]Wuppertal University, Wuppertal, Germany
[30]National Centre for Atmospheric Science, NCAS-Climate, Cambridge, UK

Received: 19 August 2009 – Accepted: 27 August 2009 – Published: 23 September 2009

Correspondence to: F. Cairo (f.cairo@isac.cnr.it)

Published by Copernicus Publications on behalf of the European Geosciences Union.

Abstract

A multi-platform field measurement campaign involving aircraft and balloons took place over West Africa between 26 July and 25 August 2006, in the frame of the concomitant AMMA Special Observing Period and SCOUT-O_3 African tropical activities.

Specifically aiming at sampling the upper troposphere and lower stratosphere, the high-altitude research aircraft M55 Geophysica was deployed in Ouagadougou (12.3° N, 1.7° W), Burkina Faso, in conjunction with the German D-20 Falcon, while a series of stratospheric balloon and sonde flights were conducted from Niamey (13.5° N, 2.0° E), Niger.

The stratospheric aircraft and balloon flights intended to gather experimental evidence for a better understanding of large scale transport, assessing the effect of lightning on NO_x production, and studying the impact of intense mesoscale convective systems on water, aerosol, dust and chemical species in the upper troposphere and lower stratosphere. The M55 Geophysica carried out five local and four transfer flights between southern Europe and the Sahel and back, while eight stratospheric balloons and twenty-nine sondes were flown from Niamey.

These experiments allowed a characterization of the tropopause and lower stratosphere of the region. We provide here an overview of the campaign activities together with a description of the general meteorological situation during the flights and a summary of the observations accomplished.

1 Introduction

Understanding the processes regulating the entry of tropospheric air into the stratosphere in the tropics is essential to assess how the stratosphere will evolve under climatic change and to deliver reliable estimates of the future ozone recovery.

The generally accepted view of troposphere to stratosphere transport in the tropics is a fast convective uplift to the level of maximum outflow of the Hadley cell at about

ACPD

9, 19713–19781, 2009

200 hPa, (Gettelman et al., 2002; Alcala and Dessler, 2002), and then slow ascent (0.2–0.3 mm/s) by radiative heating across the Tropical Tropopause Layer (TTL) (Highwood and Hoskins, 1998). The TTL shares tropospheric and stratospheric characteristics between the level of zero net radiative heating (Gettelman et al., 2004; Corti et al., 2008) and that of the cold point, or of the maximum altitude influenced by the troposphere around 70 hPa as suggested by Fueglistaler et al. (2009). A still-open question is how much fast convective overshooting of adiabatically cooled tropospheric air well above the tropopause then mixing with stratospheric air, as proposed by Danielsen (1982, 1993), contributes to the composition of the lower stratosphere.

From past observations above oceanic regions, where most high-altitude aircraft and sonde measurements are available, such overshooting events are generally assumed to be rare and therefore their contribution unimportant on a global scale.

However, as shown by geographic distribution of overshooting features seen by the precipitation radar and of flashes seen by the Lightning Imaging Sensor both on the Tropical Rainfall Measuring Mission (TRMM) satellite (Liu and Zipser, 2005), convective overshooting is by far more frequent and intense over tropical land areas where few observations are available, than over oceans. Furthermore, according to Zipser et al. (2006), most extreme events are occurring over Africa, in the equatorial region during the Northern Hemisphere winter and in the Sahel in the summer, where in situ measurements in the TTL were totally absent.

Though not yet in Africa, some aspects of the impact of tropical continental convection on the UTLS have been already explored during the EU funded projects HIBISCUS (Pommereau et al., 2007; Nielsen et al., 2007) and TROCCINOX (Chaboureau et al., 2007; Corti et al., 2008) balloon and high-altitude M55 aircraft campaigns in Brazil in 2004-2005 and during the SCOUT-O_3 M55 aircraft deployment in Northern Australia (http://www.ozone-sec.ch.cam.ac.uk/scout_o3/) (Schiller et al., 2008; Corti et al., 2008).

Among their results is the observation of fast uplift of adiabatic cooled tropospheric air and ice crystals across the tropopause over deep overshooting systems developing

in the afternoon over land, resulting in the hydration, rather than the dehydration, of the lower stratosphere, a process successfully captured by Cloud Resolving Models (Chaboureau et al., 2007; Grosvenor et al., 2007). Although the impact of such land systems on the global scale is still unclear, there are indications from zonal distributions of tropospheric tracers, such as N_2O, CH_4 and CO observed by satellites, of an increase in the concentration of these species above the tropopause over land tropical areas during the convective season, particularly intense over Africa (Ricaud et al., 2007).

Within this scientific context, the existence of another international and EU supported project, the African Monsoon Multidisciplinary Analysis (AMMA, http://science.amma-international.org) (Redelsperger et al., 2006) planning a field campaign during the summer convective season in 2006 in West Africa, offered a unique opportunity for SCOUT-O_3 scientists to extend their observations to that continent. The decision was thus made by SCOUT-O_3 to conduct balloon observations in the UTLS in the region in collaboration with AMMA during the Special Observing Period (SOP) of that project, July–August 2006 (Lebel et al., 2009), providing the first such measurements in that region. Given this unique opportunity, the decision was made by SCOUT-O_3, AMMA, the Geophysica-EEIG (European Economic Interest Group), INSU and CNRS in France to add a deployment of the M55 Geophysica during the same period. Combined together, the two projects provided the possibility of measurements during the convective season from the boundary layer to the lower stratosphere.

For practical reasons, the operations were split between Niamey (13.5° N, 2.0° E) in Niger and Ouagadougou (12.3° N, 1.7° W) located 400 km southwest of Niamey in Burkina Faso. The balloons and the FAAM BAe-146, CNRS Falcon F-20 and ATR 42 aircraft operated from Niamey airport, and the M55 and the AMMA DLR Falcon-20 were deployed at the air force base 511 of Ouagadougou. Met briefings and decision meetings for collaborative flights were conducted in teleconference between the two sites, using a Rapid Developing Thunderstorm (RDT) product based on MSG images developed by Meteo-France for following the evolution of MCS every 15 min, available

to all (Morel and Senesi, 2002). Also available in Niamey were four daily radio-sondes of a US Atmospheric Radiation Measurement (ARM) mobile facility in July–August, reinforced to eight daily from 1–15 August, and a C-band radar of the Massachussets Institute of Technology (MIT) (Williams et al., 2009). Two radio-sondes per day were also available in Ouagadougou operated by the Direction de la Meteorologie Nationale as well as a C-band radar run by the Air Force.

Ten balloons were flown between 26 July and 25 August from Niamey operated by the Centre National d'Etudes Spatiales (CNES) balloon division, complemented by 29 heavy sondes directly operated by the scientists, carrying several instruments. The M55 and the DLR Falcon F-20 performed six local flights between 1–16 August 2006, both aircraft focussing on the sampling of the middle and high troposphere and the stratosphere up to 20 km altitude, followed by the local C-band radar allowing the mission scientists to monitor and direct in real time the aircraft during their missions.

Details about the coordinated deployment of the five aircraft can be found in Reeves et al. (2009), and Lebel et al. (2009). The present paper focuses on the description of SCOUT-O_3 balloon and M55 aircraft activities. Their use in the framework of this campaign called SCOUT-AMMA, largely built on the experience of the HIBISCUS and TROCCINOX projects that took place in February 2004 and 2005 in South-America (Pommereau et al., 2007; Huntrieser et al., 2008), and the SCOUT-O_3 M55 aircraft campaign in Darwin (Australia) in November–December 2005 (Brunner et al., 2009).

This paper provides an overview of the whole SCOUT-AMMA campaign and highlights of some of its results, the details of which could be found by the reader in relevant papers. It is organized as follows: Sect. 2 is devoted to a description of the meteorology of the region associated with the monsoon, followed in Sects. 3 and 4 by a description of the aircraft and balloon payloads and flights, highlights of some of the scientific results in Sect. 5 and conclusions in Sect. 6.

2 Meteorological background

An overview of the monsoon mechanism in West Africa is given by Hall and Peyrille (2006), while a comprehensive analysis of the large and regional scales features of the summer 2006 monsoon, in relation to its interseasonal and interannual variability can be found in Janicot et al. (2008). Here is a summary of the meteorology of West Africa in the summer and its evolution during the 2006 season, with emphasis on the upper troposphere and lower stratosphere.

The vast subsidence over the Sahara desert, stronger in winter and spring, is displaced in the summer to the South-West toward the Gulf of Guinea by the developing Walker circulation, which is triggered by the Indian Monsoon outflow. Still in the summer, the air over the Sahara is subsiding in the mid to high troposphere, while intense surface heating creates a "heat low" promoting surface convergence and low to mid tropospheric divergence. This ascending region is named the Saharan Air Layer (SAL). A meridional circulation is set up with dry, warm, dust laden northerly winds moving south and overriding the moist southerly winds from the Gulf of Guinea. The region of confluence of these two currents is named the Inter Tropical Front (ITF) and moves northward as the monsoon circulation becomes established. To the south, the Inter Tropical Convergence Zone (ITCZ) follows the ITF northward.

A distinct feature of the African Monsoon is the presence of the dry and warm SAL capping the moist and relatively cool air from the Gulf of Guinea, between the ITF and the ITCZ, and thus inhibiting convection. Thus only relatively large scale systems are energetic enough to break through this air layer (Parker et al., 2005a). Hence in the Sahel, the majority of convection and rainfall is associated with large scale Mesoscale Convective Systems (MCS), forming over the Sahel and migrating westward with the mean flow. The ascending branch of the Hadley cell is situated north of the equator in summer. Upper level air moving south is deflected by the Coriolis force and acquires a westward component, forming the Tropical Easterly Jet (TEJ) situated at 16 km and 10° N over the African continent and the Gulf of Guinea.

ACPD
9, 19713–19781, 2009

Another particular feature of the general circulation over West Africa is due to the peculiar thermal structure of the region, with surface temperatures increasing and mid-tropospheric temperatures decreasing northward. This induces an easterly vertical wind shear at lower levels, and a westerly wind shear above. The surface monsoon westerlies are thus overlain by easterlies peaking at about 650 hPa, forming a seasonal easterly jet named the African Easterly Jet (AEJ), located between 5° and 15° N. This is the region where the African Easterly Waves (AEW) develop near the jet level, modulating the monsoon variability and rainfall, and eventually providing precursors for tropical cyclones over the Atlantic ocean.

The monsoon starts in the second half of June, with the ITF moving northward and crossing 15° N while the ITCZ follows by the end of June. The peak zonal-mean rainfalls migrate north from the coast of the Gulf of Guinea to the Sahel rapidly in late June (Sultan and Janicot, 2000), and retreats more slowly back again in September, promoting two rainy seasons in the south and one in the north.

2.1 The 2006 monsoon season

The 2006 season was characterized by normal convective activity, although slightly delayed and higher in July–September with respect to the mean, with excess rainfall in the northern Sahel.

Monsoon onset occurred late with respect to the long term mean: the ITCZ moved north of 10° N in the second week of July. Periods of intense AEW activities happened during the second half of July and from 15 August through mid September. Events of dry extra-tropical air intrusions originating from the polar jet and subsiding to the mid troposphere were also documented, modulated by the AEW on a 10–20 day timescale and by the Madden-Julian Oscillation (MJO) activity over the Indian region on a 40–50 day timescale. These were observed mainly in June and July and during the third week of August.

Figure 1 shows the accumulated rainfall for 1–10 August 2006. During the third decade of July, significant rainfall occurred east of Sudan, on the border between Chad

ACPD
9, 19713–19781, 2009

and the Central African Republic and over the coasts of Guinea. Precipitation intensified and extended from southern Chad to Nigeria and Cameroon during the course of the first twenty days of August. In the relatively drier sub-saharan region, only the mountain ridges in N-E Mali, N-W Niger and N Chad received significant rainfall.

2.2 Upper troposphere – lower stratosphere (UTLS)

The average ECMWF reanalyzed wind speed (m/s) and direction (vectors) at 150 and 70 hPa over Africa between 10° S and 30° N from 15 July to 16 August are shown in Fig. 2 where the TEJ can be seen with maximum intensity over East Africa. The wind speed decreases westwards being fully zonal at 5° N and diverging south and northwards.

A zonal wind vertical cross section along the 5° E meridian is shown in Fig. 3. The low altitude AEJ is centred at 5° N, while the TEJ axis shifts from 5° N at its lower levels around 200 hPa to 15° N at 80 hPa. Also shown is the stratospheric westward phase of the Quasi Biennal Oscillation (QBO) at 50 hPa at the equator and the sub-tropical and tropical westerly jets at 200 hPa at 35° N and 10° S respectively. Equatorial Kelvin waves originating from the Pacific travelling eastwards, sub-equatorial Rossby waves travelling westwards, enhanced MJO activity in the Indian and West Pacific sector, and increased convection in phase with Kelvin waves in June are documented by Janicot et al. (2008).

A reversal of the QBO winds was occurring in the lower stratosphere at the time of the SCOUT-AMMA activities. The impact of Kelvin waves on the zonal average stratospheric temperature variance of ECMWF operational analyses within 15° S–15° N is displayed in Fig. 4. The procedure for deriving the Kelvin wave component from the temperature variance employs a spectral analysis as outlined in Ern et al. (2008). The figure also shows the average ECMWF tropical zonal wind. The zero line separating east and west phase QBO is around 20 km during SCOUT-AMMA. The amplitude of Kelvin wave activity in the westerly phase is relatively small, while westward propagating equatorial Rossby waves are favoured. This is further illustrated in Fig. 5,

ACPD
9, 19713–19781, 2009

showing the ECMWF temperature anomaly at (13° N, 0° E) in July–August 2006 where the largest temperature fluctuations, of 2 K, are observed in the TTL region.

The results of a space-time spectral analysis with band pass filters corresponding to different wave modes are shown in Fig. 6, where temperature anomalies attributed respectively to Kelvin, equatorial Rossby and Rossby-gravity waves are separated. Both Kelvin and Rossby wave ridges display descent (as expected), sometimes eliding each other. Other wave modes are weaker. The amplitude of Kelvin waves is decreasing from early July to August, while that of Rossby waves increases.

2.3 Local meteorological conditions

During 2006, four daily radiosondes, reinforced to eight between 1–15 August, were launched from Niamey by the Direction de la Mètèorologie Nationale (DMN) of Niger in collaboration with the Atmospheric Radiation Measurements (ARM) Mobile Facility (AMF) (Slingo et al., 2008; Parker et al., 2009).

The mean temperature and zonal and meridional wind speed profiles and their variability (10- and 90-percentiles) over Niamey derived from the 1 July–31 August period are shown in Fig. 7. A similar analysis from the two daily sondes in Ouagadougou has been carried out providing very consistent results, but of coarser temporal resolution and is therefore not shown. On average, the Cold Point Tropopause (CPT) of 195 K is located at 375 K potential temperature, 500 m above the Lapse Rate Tropopause (LRT) at about 16 km. The equilibrium level, the altitude at which the lapse rate starts to increase, is around 14 km. The temperature is most variable in the boundary layer and in the UTLS above the LRT where the amplitude of the deviation reaches ±7 K at the CPT. With the exception of the monsoon south-westerly flow near the surface, the wind is nearly zonal and easterly at all levels. Evident on the rightmost panels of Fig. 7 are the monsoon south-westerly flow near the surface, the AEJ peaking at 4 km of 12 m/s mean core speed corresponding to a layer of reduced stability, and the TEJ peaking around the tropopause at a speed of 15 m/s.

ACPD
9, 19713–19781, 2009

Figure 8 shows the time series of temperature anomaly relative to the campaign mean. Added on the figure are the altitudes of the CPT (white squares) and of the 340 K and 365 K isentropic surfaces (black squares). The pronounced wave-fronts in the stratosphere that are descending in time are structures common to the Ouagadougou time-series (not shown) and thus the result of large scale tropical wave activity. Their amplitude of 8 K is larger than that the 2 K derived from ECMWF reanalysis shown in Fig. 5, suggesting that the latter is not fully capturing these waves.

Figure 9 shows the result of a spectral analysis of the temperature anomaly. The presence of a diurnal cycle is obvious at all levels but of largest amplitude in the surface layer and above the tropopause, then a 3–4 day period in the troposphere, and then longer modulations of 10 days or longer periods associated with Kelvin and Rossby waves.

Figure 10 shows the amplitude and the phase of the average daily change of temperature compared to its noon value at 900, 600, 150 and 80 hPa. The lower layer near the surface displays an average warming of 5 K through the day due to the solar heating, combined with advective cooling by the monsoon at night (Parker et al., 2005b). The mid-troposphere (600 hPa) and equilibrium (150 hPa) levels show only a small warming of less than 1 K in the afternoon, where the adiabatic cooling of convectively lifted air is compensated by the release of latent heat by precipitation. Most remarkable is the average afternoon cooling at 80 hPa, that is 1.5 km above the CPT, of 2 K amplitude at sunset compared to the early morning. This diurnal cycle in the lower stratosphere is very similar to that observed by Pommereau and Held (2007) in southern Brazil during the convective season coincident with the diurnal cloud top altitude modulation and attributed to an injection of adiabatically cooled air by deep overshooting across the tropopause as proposed by Danielsen (1993). A detailed examination of these series of the soundings is not the purpose of this paper, but important here is the confirmation of the existence of deep overshooting in the lower stratosphere above West Africa during the summer season.

ACPD
9, 19713–19781, 2009

3 M55 Geophysica, balloons and sondes payload

3.1 Geophysica payload

The stratospheric research aircraft M55 Geophysica is described by Stefanutti et al. (1999). The Geophysica was instrumented with a comprehensive payload for in-situ microphysical and chemical measurements as well as spectrometers for remote trace gas measurements.

As some instruments shared the same bay, not everyone of them could be flown on the same mission. The definition of the optimal payload was decided according to the objectives of the specific flights. Table 1 lists the instruments and the flights in which they were deployed. In the following, a short description of each instrument is presented.

MAS (Multiwavelength Aerosol Scatterometer) is a backscattersonde (Buontempo et al., 2006; Cairo et al., 2004) that measures in-situ the optical parameters of the airmass, as volume backscatter ratio and depolarization ratio at 532 nm and 1064 nm, so it acts as a detector of cloud particles and aerosols, able to discriminate their shape, i.e. phase, by polarization measurements. It has a time resolution of 5 s, a precision of 5% and an accuracy of 0.05 on the backscatter ratio. A smaller version of this instrument, LABS has been deployed on balloons as well.

FISH (Fast In situ Stratospheric Hygrometer) is a Lyman-alpha hygrometer to measure total water content with a precision of 6%+0.15 ppmv and an accuracy of 0.15 ppmv, and a time resolution of 1 s (Zöger et al., 1999). The oversampling of condensed water inside clouds is corrected as described in Schiller et al. (2008).

FLASH-A is a Lyman-alpha hygrometer to measure water vapour with a 1 s resolution, an accuracy of 0.2 ppmv and a precision of 6%. A ballon-borne version of this instrument has also been deployed during the campaign, and is described in more detail in 3.2 (Yushkov et al., 1998).

FOZAN (Fast OZone ANalyser) is a fast response ozonometre which is based on a chemiluminescent reaction between a dye and the ambient ozone. It has a time

resolution of 1 s, an accuracy of 0.01 ppmv and a precision of 8% (Yushkov et al., 1999).

HAGAR (High Altitude Gas AnalyzeR) is a gas chromatograph to detect long-lived tracers (N_2O, CFC-12, CFC-11, Halon-1211, H_2, SF_6, CH_4, CO_2) with a time resolution of 90 seconds and accuracies between 2% and 4% depending on the species. An additional non-dispersive IR analyzer provides CO_2 measurements with a time resolution of 5 s and an accuracy of 0.1% (Volk et al., 2000).

SIOUX (StratospherIc Observation Unit for nitrogen oXides) is a two-channel instrument for measurements of nitric oxides (NO), total reactive nitrogen (NO_y) and NO_y contained in particles larger than 1 μm in diameter (Schmitt, 2003; Voigt et al., 2005), The detection of NO relies on NO/O_3-chemiluminescence. Higher oxidised NO_y species are reduced to NO prior to detection using a heated Au-converter and CO gas as catalyst. Particle-phase NO_y is measured by oversampling of particles in a forward facing inlet and evaporation and reduction of NO_y species (mainly HNO_3) in the heated inlet and AU-converter. The accuracy and precision of the measurements are 5%–10% (NO) and 7%–15% (NO_y).

ALTO (Airborne Laser Tunable Observer) is a Near InfraRed tunable diode laser spectrometer for absolute measurements of Methane (CH_4) concentration with a time-resolution of 5 s, a sensitivity of 60 ppbV, an accuracy of 15% and a precision of 5% (D'Amato et al., 2002).

COLD (Cryogenically Operated Laser Diode) is a Middle InfraRed tunable diode laser spectrometer for absolute measurements of Carbon Monoxide (CO) concentration with a time-resolution of 4 s, a sensitivity of 3 ppbv, an accuracy of 6–9% (due to the accuracy of molecular database) and a precision of few % (Viciani et al., 2008).

IRIS (Kerstel et al., 2006) is a compact and cryogen-free, cavity-enhanced spectrometer for the in-situ measurement of water vapor isotopes. Precisions are about 9%, 20%, and 100% at a 1-s time resolution and a mixing ratio of 100 ppmv, for delta18O, delta17O, and delta2H, respectively. Longer averaging of the data should enable the same level of precision to be maintained all the way down to stratospheric

ACPD
9, 19713–19781, 2009

water concentration levels.

HALOX is a chemical conversion resonance fluorescence sensor for the in-situ measurement of the HALogen OXides ClO and BrO (von Hobe et al., 2005). For the low halogen oxide mixing ratios encountered in the tropical UTLS integration times of around 5 to 30 min are required. ClO can be measured from as low as 10 km and BrO from around 16 km with lower detection thresholds of 1–2 pptv. An accuracy of better than 20% (or 2 pptv, whatever is higher) for ClO and 35% (or 2 pptv, whatever is higher) for BrO is obtained. Precision of the measurements is as good as 10% but increases considerably for shorter integration times.

The payload of the Whole Air Sampler (WAS) can be alternatively equipped with a Whole Air Sampler (WAS-1) or a Water Sampler (WAS-2). WAS-1 compresses ambient air into 2 L evacuated stainless steel flasks to a pressure of 450 kPa, which are then routinely analyzed for the isotopic composition of the long-lived trace gases CH_4 and N_2O (Kaiser et al., 2006) and in the SCOUT-O_3 project for halogenated species (Laube et al., 2009). WAS-2 is a cryogenic sampler that samples atmospheric water vapour for subsequent isotope analysis in the laboratory (Franz and Röckmann, 2005).

MIPAS, the Michelson Interferometer for Passive Atmospheric Sounding, is a mid-infrared emission spectrometer which is an airborne version of the one on board the ENVISAT satellite. It is a limb sounder able to retrieve vertical temperature, trace species and cloud distributions. The instrument is a well calibrated and characterized Fourier transform spectrometer which is able to detect many trace constituents, as H_2O, O_3, CH_4, N_2O, HNO_3, and NO_2 (Fischer et al., 2008).

CRISTA-NF (CRyogenic Infrared Spectrometers and Telescopes for the Atmosphere – New Frontiers) is a Mid-IR limb emission instrument installed onboard M55-Geophysica (Spang et al., 2008; Hoffmann et al., 2009). It's measurements allow for retrievals of temperature, H_2O, O_3, HNO_3, PAN, CCl_4 as well as aerosol and cloud optical properties with vertical and horizontal resolutions on the order of a few 100 m and a few kilometers in the altitude range 6 to 20 km.

COPAS is a four channel COndensation PArticle measurement System specifically designed for deployment in the UTLS on the M-55 Geophysica. COPAS detects and counts aerosol particles (without size determination) larger than 6 nm, 10 nm and 14 nm respectively, in order to measure particle number densities. The fourth channel heats the sampled air to 250°C prior to the aerosol detection this way measuring the number concentration of non volatile particles having sizes above 10 nm. The upper size detection limit of all channels is roughly 1 μm (Weigel et al., 2008; Curtius et al., 2005) as determined by the sampling inlet. The data acquisition rate is 1 Hz resulting in horizontal and vertical resolutions of roughly 200 m and 10 m from the ground to 20 km altitude. However for reasons of counting statistics during most flights 15 or 30 s flight time averages of the data are reported.

CIP is the Cloud Imaging Probe from Droplet Measurement Technologies Inc. (DMT, Boulder, Colorado, USA) which has been modified for the specific operating conditions of Geophysica. It is a two dimensional optical array probe recording shadow cast images of individual cloud particles by means of a linear array of 64 light detectors and a laser light source. The CIP detects and sizes large aerosol particles and cloud hydrometeros with diameters between 25 μm and 1550 μm and thus is well suited for deployment in cirrus and subvisual cirrus clouds. At 190 ms^{-1} travelling speed of Geophysica its scanning rate over the diode array is 7.6 MHz resulting in a particle size resolution of 25 μm. The extraction of the size information from the recorded images is performed using the minimum and the maximum dimensions of the particles and applying various corrections (DeReus et al., 2008).

FSSP-SPP-100 and -300 measure the forward scattered laser light of single particles within a scattering angle of 4°–12° this way covering particle size diameters between roughly 0.3 μm and 31 μm (FSSP-SPP-300) and 2.7 μm and 30 μm (FSSP-SPP-100). Using Mie-calculations, the size of a particle is related to the measured scattering cross section, which implicitly assumes spherical particles. However the instruments can also be applied for aspherical particles, if these are smaller than 23 μm (Borrmann et al., 2000). The particle size distributions initially consist of 40 size bins

but this resolution usually is reduced to below 10 bins based on Mie-ambiguities and counting statistics. The uncertainties of the number concentrations reported by the FSSP are determined by the uncertainty of the sample volume (approximately 20%) and mostly counting statistics at low number densities like in thin or subvisual cirrus clouds (Thomas et al., 2002). For these reasons the 2 s accumulation interval data records on Geophysica result in decreased resolutions of typically 30 s to several minutes of flight time. The instruments have been modified by implementing digital signal processor electronics (DMT Inc, Boulder, Colorado, USA) and specific changes necessary for the ambiental conditions encountered in the UTLS with Geophysica.

For in situ measurements at a flight level of atmospheric pressure, ambient air temperature, wind speed, the russian Central Aerological Observatory (CAO) developed, and the Experimental Engineering Plant manufactured, an autonomous thermodynamic complex (TDC). The complex includes high-precision sensors and converters made by Rosemount company and a unit that collects, processes, and records information, operating in the interactive regime with standard measuring and navigation aircraft systems, and stores the information on measured and computed thermodynamic parameters in the energy-independent memory (Shur et al., 2007).

3.2 Balloons payload

The balloons launched from Niamey airport were of two types: 3000–12 000 m^3 balloons flown for 3–4 h operated by the team of the French Centre National d'Etudes Spatiales (CNES) with the help of the Nigeran Air Force for payload recovery in Burkina Faso, and smaller 1500–4000 m^3 plastic balloon sondes operated by the scientists. The instruments available for the balloons were: a micro-DIRAC gas chromatograph for the in situ measurement of halogen species, a micro-SDLA tunable diode laser hygrometer, a SAOZ UV-Vis spectrometer for remote measurement of ozone, NO_2, H_2O and aerosols extinction, a SAOZ UV version for the remote measurement of BrO, a micro-lidar and a global IR radiometer for cloud detection, a LABS diode laser for aerosols and clouds, an optical particle counter (OPC) for the size distribution of the

ACPD
9, 19713–19781, 2009

particles, a NILUCUBE for radiation, lightning optical detectors and finally a HV-AIRS vertical electric field probe. Those available for the sondes were backscatter-sonde (BKS) for aerosol and particles, FLASH-B Lyman alpha hygrometers and commercial ozone sensors. They are all described shortly below.

Micro-DIRAC (Determination In situ by Rapid Analytical Chromatography) is a lightweight version (10 kg) of the DIRAC gas chromatograph developed by the University of Cambridge described by Robinson et al. (2000) and Gostlow et al. (2009). It uses a carboxen adsorbent to pre-concentrate samples of known volume before injection onto a separation column and electron capture detector. It measures a range of halocarbons at a time resolution, which can be adjusted depending on the type of flight being made. For instance, CFC-11 and CFC-113 can be measured at 100-s intervals (0.3–0.7 km resolution depending on balloon vertical velocity) or CFC-11, CFC-113, $CHCl_3$, CH_3CCl_3 and CCl_4 can be measured at 200-second intervals (0.6–1.4 km resolution). It has been successfully deployed on 10 balloon flights in the past. The repeatability of standard gas measurements during flight (1 sigma in-flight precision) is 6.5% for CFC-11, 7.5% for CCl_4, 10% for CH_3CCl_3 and 15% for $CHCl_3$.

The micro-SDLA sensor of CNRS and University of Reims Champagne-Ardennes (URCA) developed with the help of Division technique de l'Institut National des Sciences de l'Univers (DT-INSU) is a tunable diode laser spectrometer devoted to the in situ measurement of H_2O, CH_4 and CO_2 by infrared absorption spectroscopy (Durry et al., 2004). Three near-infrared telecommunication-type InGaAs laser diodes are connected by means of optical fibres to an open multi-path optical cell providing an absorption path-length of 28 m. The laser beam is absorbed by ambient gas molecules as it is bouncing back and forth between the cell mirrors. CH_4 is monitored at 1.65 μm, CO_2 at 1.60 μm and H_2O at 1.39 μm using the differential detection technique. The payload also includes pressure and temperature sensors. The accuracy of the H_2O measurements within 160 ms is 5%. Micro-SDLA was already flown successfully in the tropics during the HIBISCUS campaign (Marecal et al., 2007).

ACPD
9, 19713–19781, 2009

The SAOZ of CNRS-SA is a UV-Vis spectrometer for remote measurement by solar occultation during the ascent of the balloon in the late afternoon and at sunset or sunrise from float altitude. Three versions have been deployed during HIBISCUS: the basic SAOZ in the 300–650 nm spectral region for O_3 (2% accuracy), NO_2 (5%), and cloud extinction (Pommereau and Piquard, 1994), a UV enhanced version in the 300–400 nm range, SAOZ-BrO, for BrO (15%) (Pundt et al., 2002), and a newly developed 400–1000 nm version SAOZ-H_2O for the measurement of H_2O in addition to O_3 and NO_2. The SAOZ payload weighs 18 kg.

The micro-LIDAR, MULID, is a lightweight low-power micro-lidar of ENEA and CNR-ISAC employing a miniaturized Nd-YAG pulsed laser firing at 532 nm for measuring profiles of aerosol backscatter and depolarization during nighttime, from the altitude of the balloon down to the ground, with a vertical resolution of 30 m and a time resolution of 60 s. In daylight conditions, the system is unable to provide profile information but operates as a near-range backscatter-sonde, providing values of backscatter and depolarization at a few tens of metres from the platform. The parameters obtained by MULID are, apart from intensity and depolarization profiles of the backscattered signal, the extinction profile in optically thin clouds and the cloud top height for optically thick clouds (Di Donfrancesco et al., 2006).

The Global IR radiometer is lightweight (160 g) sensor developed by CNRS-SA following a design proposed by Suomi et al. (1958), for detecting the evolution of the cloud cover below the balloon.

The balloon-borne LABS of CNR-ISAC and ENEA is a single wavelength (532 nm) lighter version of the MAS instrument, already described in the M55 payload.

The Optical Particle Counter of the University of Wyoming (Deshler et al., 2003) measure forward scattering, using dark field microscopy, to size and count aerosol particles in the sample stream. Two instruments are usually deployed, a condensation nuclei counter (CN) to measure the concentration of all particles $\geq$0.01 μm, and a size resolving counter for particles between 0.15 and 10.0 μm in 12 channels. The size precision is 10% and the concentration precisions determined by Poisson counting statistics for

ACPD
9, 19713–19781, 2009

low concentrations and a minimum of 10% at high concentrations. The altitude range is surface to balloon burst, typically 30 km. The CN counter uses ethylene glycol in a growth chamber to force the particles to grow to optically detectable sizes. These instruments have been flown throughout the world and have a long history (Deshler et al., 2006).

The NILUCUBE is a lightweight multi-channel moderate bandwidth filter instrument (Kylling et al., 2003) of the Norwegian Institute for Air Research. It consists of six heads mounted on each of the faces of a cube. For this particular campaign each head measured UV radiation at centre wavelengths of 301, 311, 317, 340 and 375 nm, with a full width half maximum (FWHM) of about 10 nm. In addition a wideband channel measuring the photosynthetic active radiation (PAR, 400–700 nm) was available. Based on model simulations of the measured radiation, actinic flux spectra and photodissociation rates can be estimated. The weight of the instrument is about 6 kg.

The HV-AIRS (Atmospheric Impact of Radiations and Sprites) of CNRS-CETP includes an electric field probe and two lightning optical sensors. The probe measures the vertical component of the atmospheric electric field. It uses the double probe technique with 2 cylindrical electrodes distant by 37 cm, resistively coupled to the atmosphere, located at both ends of a small vertical boom 25 cm from the gondola. Electrically grounded metallic plates on the side of the gondola provide a reference surface in contact with the ambient ionized atmosphere, which is much larger than the surface of the electrodes. The high input impedance and low leakage currents preamplifiers connected to the electrodes allow to measure electric fields above ~8 km altitude. DC and large amplitude signals from 0 to ~4 kHz and up to ±110 V/m are measured in the so-called "DC channel" with a resolution of ~12 mV/m. Small amplitude AC signals between 4 Hz and 4 kHz with amplitude less than 1 V/m are measured in the so-called "AC channel" with a sensitivity threshold of 30 μV/m. Positive and negative electric conductivities of the atmosphere in the range 5×10^{-14} S/m and 10^{-11} S/m are determined alternately every 4 min using the instrument in the relaxation mode.

ACPD
9, 19713–19781, 2009

The lightning optical sensors built by CNRS-SA are designed for detecting lightning flashes below the balloon and eventually Transient Luminous Events (TLE) such as blue-jets above. The sensors are made of a photodiode and an amplifier with the lightning detector looking downward within a 180° FOV and the TLE detector upward within a 30–80° annular FOV to avoid reflection of lightning flashes on the balloon. These optical detectors are saturated by the solar flux and only work after sunset.

All HV-AIRS data are stored in an on-board memory that provides the high time resolution that is needed to study lightning induced phenomena.

3.3 Sondes payload

The backscatter-sonde (BKS) and ozonesondes operated by the Danish Meteorological Institute make use of a Wyoming backscatter sonde (Rosen and Kjome, 1991), made of a xenon lamp, which emits a white flash every 7 s. The light is scattered by particles and molecules in front of the sonde, and monitored with two photodiodes at 480 and 940 nm, respectively. Two parameters are calculated from this signal: the backscatter ratio (BR), i.e. the ratio between the observed backscatter coefficient and the calculated molecular backscatter, and the color index, defined as (BR940-1)/(BR480-1). The color index is correlated with the particle size. The ozone sondes are commercial Electro Chemical Cells from ENSci mounted on a RS92 Vaisala radio sonde. Ozone, pressure and temperature are measured simultaneously.

The FLASH-B (FLuorescence Advanced Stratospheric Hygrometer for Balloon) instrument is the Lyman-alpha hygrometer developed at the Central Aerological Observatory for balloon water vapour measurements in the upper troposphere and stratosphere (Yushkov et al., 1998). The instrument is based on the fluorescent method (Kley and Stone, 1978), which uses the photodissociation of H_2O molecules at a wavelength ≤137 nm followed by the measurement of the fluorescence of excited OH radicals. The source of Lyman-alpha (at 121.6 nm) is a hydrogen discharge lamp, while the detector of OH fluorescence at 308–316 nm is a photomultiplier run in photon counting mode. The intensity of the fluorescent light sensed by the photomultiplier

ACPD
9, 19713–19781, 2009

is directly proportional to the water vapour mixing ratio under stratospheric conditions (10–150 hPa). Because of the Lyman alpha absorption and the open optical layout, the measurements are limited to pressure lower than 300–400 hPa and solar zenith angle larger than 98°. The hygrometer is coupled with a Vaisala RS-80 radiosonde providing telemetry, pressure and temperature measurements. The sampling is of 4 s corresponding to a vertical resolution of 20 m during ascent and 100 m during the fast 15 m/s descent around the tropopause. To avoid contamination FLASH-B is mounted at the bottom of the flight train 40 m below the balloon. Descent data only are being used.

4 M55 Geophysica, balloons and sondes flights

4.1 Geophysica flights

The aircraft was instrumented in Verona, Italy (45.4° N, 10.9° E) from where it left on the 31 July 2006 for Ouagadougou, arriving on 1 August, after an intermediate stop in Marrakesh, Morocco (31.63° N, −8.00° E). It performed five scientific local flights from Ouagadougou during the first half of August, then left for the return trip on 16 August, following the same transfer route with intermediate stop in Marrakesh and reached Verona on the 17 August.

In the following a description of the flights over the Sahel, the two transfer flights Marrakesh-Ouagadougou and the transfers Verona-Marrakesh is given. The five local flights were designed according to five different templates, specifically to (I) perform survey flights in conditions as unperturbed as possible by convection; (II) to sample air affected by recent and (III) by aged convection, (IV) to investigate the long range transport across a meridional transect, and finally (V) to validate the satellite borne Cloud-Aerosol LIdar with Orthogonal Polarization (CALIOP) lidar cloud products. A list of the payload and data availability for these flights is reported in Table 1.

4.1.1 31 July 2006 (Julian Day 212), Verona-Marrakesh transfer flight

The Geophysica left Verona at 23:26 LT (21:26 UTC) arriving in Marrakesh at 01:17 LT (01:17 UTC) roughly following the south-west European and African coastline. In order to perform a remote sensing of the UTLS region from middle to low latitudes, the flight was planned to provide optimal performance for the spectrometers on board, i.e. at the maximum altitude compatible with the route safety concerns. A first leg at 17.5 km altitude lasting one hour was followed by a second leg at 18.5 km, until the destination. The weather on the route was fine and with clear sky.

4.1.2 1 August 2006 (Julian Day 213), Marrakesh-Ouagadougou transfer flight

The aircraft took off at 10:59 UTC following a straight flight path with two constant altitude legs at 17.5 km and 18.5 km to Ouagadougou, crossing the Sahara and Sahel regions which had not been recently affected by convection. During the first leg of the flight, at 82 hPa over the desert, (i.e. approximately 410–420 K potential temperature) very low values of N_2O were observed together with an enhanced non volatile fraction of CN, with respect to the campaign average values. On the second leg, at 68 hPa (440–450 K) values of tropospheric tracers as CFC-11 and CFC-13 indicated ages of air peculiar and different to what will be observed in the later flights of the campaign. Part of the flight track is shown in Fig. 11, panel a. On the same first leg, an enhancement of CO_2 and CN non volatile fraction, in the potential temperature layer between 390 K and 420 K, was observed, together with a slight enhancement of the overall CN on the same layer. Stratospheric tracers like N_2O show deviations from their average values taken subsequently during the campaign. During the second leg, all the stratospheric tracers showed deviation from the campaign average profiles, indicating airmasses of non tropical origin.

ACPD
9, 19713–19781, 2009

4.1.3 4 August 2006 (Julian Day 216), Long range transport

The aim of the flight was to sample the TTL region along a north-south transect to cross the latitudinal gradient of the region likely to be affected by the general transport. In particular, it aimed to measure the long range transport from the summer monsoon circulation over Asia into the TTL over West Africa in order to compare it with the influence of local convection. So, this flight tried to take place when MCS activities in the region were at a minimum. There was no convection predicted for the day in the region where the mission took place. Nevertheless, convection which could have influenced the measurements was present the evening before over Ghana and on the morning of the mission over the western part of Burkina Faso, moving westward. The flight profile was designed to have constant level legs and vertical profiles from 19 to 12 km at the final points of the transect, over the Guinea Gulf coasts, to acquire full vertical profiles of atmospheric constituents. The plane took off at 08:26 UTC heading southward at a constant altitude of 16 km. Before reaching the southernmost point over the Gulf of Guinea, it performed an altitude excursion climbing at 19 km and descending down to 12 km, before turning back and heading northward at a constant altitude of 15 km. In proximity of Ouagadougou, a climbing up to 19.5 km was performed followed by the final descent to land at 12:13 UTC. The flight track is shown in Fig. 11, panel b. The F-20 Falcon performed a flight at the same time, following a similar geographical pattern at lower levels. On the first leg at constant level between 370 K and 380 K, in a region free of clouds and rather dry, an enhancement of the CN ultrafine mode fraction was observed but with no concomitant enhancement of total CN, while CO_2 and O_3 were at their average values. Then, at the top of the ascent in proximity of the Guinea Gulf coast, in an airmass clear of clouds and rather dry, a slight enhancement of total CN was observed, with a very low ultrafine mode fraction and a low non-volatile fraction. On the dive down to 350 K, still in a region free of clouds and rather dry, enhancements and large variability of the total CN and of its non-volatile fraction were observed, while a high ultrafine mode fraction was also present. At the same time, O_3

ACPD
9, 19713–19781, 2009

was slightly enhanced, while CO_2 seemed largely variable, and slightly enhanced in a layer around 370 K.

4.1.4 7 August 2006 (Julian Day 219), MCS close-up

The flight on the 7 August attempted a MCS close-up. The MCS originated in the night over central Mali, developed overnight slowly moving south-westward. The MCS evolution was monitored in real time by continuous inspection of MSG images. The aircraft took off at 12:15 UTC, chasing the system as it moved westward and reaching its back and wake over southwest Mali. Unfortunately the more active part of the system had already passed over. The aircraft performed frequent altitude excursion during the ferry legs and when in the region of the MCS wake where cloudiness was present below and the presence of a cloud tower to the left of the aircraft was reported. As the aircraft turned northward, it performed a dive from 18 km to 12 km, then climbed up to the ceiling altitude of 19.5 km before leaving the MCS wake area. In the lowermost part of this altitude excursion, it entered into layered clouds and the pilot reported light turbulence. It then got back eastward and landed in Ouagadougou at 16:07 UTC. The flight track is shown in Fig. 11, panel c. The F-20 Falcon flew at the same time, following a geographical pattern slightly displaced northward with respect to the M55, sampling the atmosphere from 8 to 12 km.

On approaching the MCS wake area, an enhancement of CO was observed between 390 K and 410 K in a region free of clouds but with a thin cloud layer below, at 370 K. At those levels, water was at the lowest values observed during the campaign. No diversions from average values of CN, but very low values of fine mode fraction were observed. The Ozone showed a layered structure, remaining slightly below its average values, while CO values were enhanced with respect to what was observed elsewhere.

On its way back, during the climbing to the ceiling altitude, an hydrated layer was observed between 380 K and 410 K in a region free of clouds but with a thin cloud below, at 370 K. CN values remained close to their averages, but very low values of fine mode fraction were observed. Ozone showed a layered structure, remaining slightly

below its average values. CO values were at the high limit of their variability. Finally, during the descent to Ouagadougou inside a layered cloud, observations of very high concentration of NO_y and NO were observed. CN concentration was on the average, while the high concentration of ultrafine particles shows the occurrence of a nucleation event. There, CO concentrations were higher than their average campaign values.

4.1.5 8 August 2006 (Julian Day 220), CALIOP validation

The flight was designed to follow the footprint of the CALIOP lidar on board the Cloud-Aerosol Lidar and Infrared Pathfinder Satellite Observations (CALIPSO) satellite, to validate its cloud products with observations of upper clouds structure and microphysics, including size and shape of ice crystals. CALIPSO is part of the A-train and follows a sun-synchronous orbit, the ascending node crossing the equator at 13:43 local time with a 16-day repetition cycle.

In the region close to Ouagadougou, daytime over-passes are for ascending orbits from South-East to North-West. The M55 was aimed to fly along the CALIPSO footprint, about 30 min before and after CALIPSO overpass with altitude excursions, to vertically sample thin cirrus clouds, while the ferry flights, and the time of flight out of the CALIPSO validation time, would have been eventually devoted to cirrus sampling in that region. The flight was designed to meet the CALIOP footprint along a line extending from 9.04° N, 2.55° E to 12.77° N, 1.77° E which the satellite was going to overpass from 13:28 UTC to 13:30 UTC. The meeting point of the two platforms was forecasted to be in the middle of this line, at 13:29 UTC.

The aircraft took off at 11:46 UTC and climbed to 17.5 km to descend to 14.5 km and perform a stepwise ferry flight with legs at 15.5 and 16.5 to reach the first intersection with the CALIOP footprint. The aircraft followed the CALIOP footprint initially at an altitude of 16.5, then just before reaching the meeting point with CALIOP, it started ascending to 19.5 km. The meeting point was reached at 13:29 UTC during the climbing. It then followed the CALIOP footprint with 100 km stepwise horizontal legs at this level, and at 18, 16, and 15 km. Upon leaving the footprint and turning to Ouagadougou,

ACPD
9, 19713–19781, 2009

a final slow climbing to the ceiling altitude of 20 km was performed. The flight track is shown in Fig. 11, panel d. High level clouds were observed in proximity of Ouagadougou and, of use for the CALIOP validation, on the last part of the footprint leg.

Between 375 and 395 K the Geophysica repeatedly probed a layer with enhanced water vapor. Thin cirrus were embedded within and below this layer as observed with the backscatter sonde, the FSSP and the CALIOP lidar instrument onboard CALIPSO.

A hydrated layer in cloud free regions was observed between 375 K and 395 K each time the aircraft crossed that layer, throughout the flight. On the last part of the CALIOP flight leg, thin layers of enhanced water were observed above the cold point, at 420 K and 400 K in cloud free air, together with a decrease of CO. In that region the temperature profile was extremely variable. Additionally large reactive nitrogen (NO_y) containing particles were observed by SIOUX and the FSSP onboard the M55-Geophysica near and below the thermal tropopause. The particles, most likely nitric acid trihydrate (NAT, $HNO_3 \times 3H_2O$) have diameters less than 6 μm and concentrations below 10^{-4} cm^{-3}. Such dilute concentrations of NAT particles are known to exist in the winter polar stratosphere (Voigt et al., 2005) and also reported in the tropics (Popp et al., 2006). The NAT particle layer was repeatedly detected between 360 and 385 K (15.1 and 17.5 km) over extended areas of 9.5 to 17.2° N and 1.5° W to 2.7° E (Voigt et al., 2008).

On the final descent to Ouagadougou, a high fraction of fine mode CN was observed, indicating a fresh nucleation event at the tropopause level between 340 K and 360 K where a thin cloud was also present. A very layered structure for Ozone was present above that level, and an enhancement of CO_2 was observed between 390 K and 400 K.

4.1.6 11 August 2006 (Julian Day 223), MCS aged outflow

This flight aimed at sampling a TTL air that was likely to have been processed by an MCS system in the previous days; one of such systems developed two days earlier over the eastern border of Nigeria, then moved north-westward extending from the Niger-Nigeria border to Benin and Togo, to continue its westward movement over Burkina

ACPD
9, 19713–19781, 2009

Faso and starting to dissipate the day of the flight. An encounter with airmasses containing aged MCS outflow was forecasted, based on MSG satellite imagery and forward trajectory calculations using LAGRANTO with a spectral resolution of T319L91. The forward trajectories were started from positions of any active MCS upwind of the investigation area identified by very low brightness temperations. On the 11th of August, aged MCS outflow was predicted for the region of the Burkina Faso-Niger-Mali borders. To sample these air masses, the Geophysica took off at 14:44 UTC heading northeast at 16.5 km, then 17.5 km altitude for the ferry part of the flight to reach the region of possible outflow. Once it reached the northernmost point, it turned twice southeast and southwestward to come back to Ouagadougou. During this part of the flight, it repatedly performed dives to 12 km and ascents to 15 km. On the last part of the light it climbed up to the ceiling altitude of 20 km before the final descent to Ouagadougou, where it landed at 18:22 UTC. During the first part of the flight, solid cloudiness was observed at an altitude of 9–10 km below the aircraft, probably remnants of the MCS passing over the Ouagadougou region. The flight track is shown in Fig. 11, panel e. The F-20 Falcon performed a flight on the same day, sampling the same region at lower levels.

On the final ascent, thin layers of enhanced water were observed above the cold point between 410 K and 420 K. Higher up, between 440 K and 490 K, thin layers of non depolarizing particles were observed and attributed to the detection of the La Soufriere Hills volcanic eruption plume (Prata et al., 2007). A slight enhancement on the water profile was also observed there. CN values were close to the campaign average, although the non-volatile fraction was slightly enhanced. CO_2 and N_2O were lower than average.

4.1.7 13 August 2006 (Julian Day 225), UTLS survey

The flight aimed at a survey of the UTLS over a meridional transect in relatively quiescent conditions, but took the advantage of a very close overpassing of the CALIOP footprint over Ouagadougou, so the flight track was planned to follow this footprint while

heading south. There was no local convective activity, although large MCS activity was occurring over Chad and the Central African Republic since the day before. Very few low level clouds were encountered while flying over the continent, while no clouds at all were present over the ocean.

The aircraft took off at 12:50 UTC and reached the CALIOP trajectory at 13:21 UTC (its overpassing was foreseen between 13:46 UTC and 13:48 UTC) which was carried out with a stepwise descent from 18.5 km down to 12 km. Then, before reaching the southernmost point of the track over the Gulf of Guinea, an ascent was made up to 18.5 km. On the way back a further stepwise ascent was performed to reach the ceiling altitude of 20 km before landing at Ouagadougou, at 16:23 UTC. The flight track is shown in Fig. 11, panel f.

During the dive, before reaching the southernmost point of the route, a slight enhancement of CO_2 with respect to its average values was observed. Once reaching the southernmost point of the flight, on ascent, large water contents were observed at the hygropause, water being enhanced throughout the profile up in the stratosphere. Conversely, Ozone was reduced in the stratosphere, compared to its average profile. The flight track is shown in Fig. 11, panel f.

4.1.8 16 August 2006 (Julian Day 228), Ouagadougou-Marrakesh transfer flight

A large MCS developed in the early morning in central Burkina Faso, and was over Ouagadougou by noon. The aircraft left Ouagadougou at 13:27 UTC when the meteorological conditions allowed to take off. It followed a straight flight at a constant level of 17.5 km to Marrakesh, where it landed at 17:16 UTC. A very low concentration of CN was encontered during ascent, from 350 K up to 365 K, level that coincided with the cold point tropopause. This low concentration coincided with a very low value of the non-volatile fraction of CN. The observation was taken inside a cloud. Fairly high presence of NO_y and low level of CO_2 were also detected. In the middle of the flight, over the Sahara desert at 420 K potential temperature, an enhancement of water vapour from its average value of 5–6 ppmv to 8 ppmv was observed for 2000 s (i.e. 400 km)

ACPD
9, 19713–19781, 2009

during level flight. Part of the flight track is shown in Fig. 11, panel g.

4.1.9 17 August 2006 (Julian Day 229), Marrakesh-Verona transfer flight

The take off was made at night at 04:10 UTC The aircraft followed the African and south European coast line, at a constant altitude of 17.7 km, in the dark for the first hour of the flight. It landed in Verona at 07:51 UTC.

4.2 Balloons and sondes flights

The concept of the campaign was to associate several payloads of compatible operational requirements below the same balloon for complementary measurements oriented toward a specific scientific objective. Because of the limited reliability of model predictions, flight decisions were made on now-casting from the information available from the AMMA Rapid Thunderstorm Development (RDT) product refreshed every 15 minutes and those of the MIT C-Band radar available every 10 min. When possible, the balloons were accompanied by a sonde as close as possible, but not before sunset because of the stray-light restriction of the BKS and FLASH hygrometer.

Four balloon templates were designed: *Ice and Aerosols*, *Water Vapour*, *Anvils and Cirrus*, and *Chemistry*.

- *Ice and Aerosols* focussed on the description of cirrus optical properties, microphysics, and transport from the PBL to the UTLS if possible in an outflow region. The payload included OPC, LABS and micro-DIRAC. The plan was to reach 22–23 km, dwell there at constant level for one hour and then descend slowly into the TTL for another 1–2 h. Two flights of this type have been made, on 31 July and 17 August. An additional flight carrying the OPC alone was performed on 31 July.

- *Water Vapour* aimed at studying troposphere to stratosphere transport triggered by overshooting deep convection with in situ measurements of water vapour, ice clouds and tracers in the lower stratosphere, if possible close to an MCS or local

convection. The flight train was formed of micro-SDLA, LABS and micro-DIRAC. The flight template foresaw a ceiling at about 25 km with a short float followed by a slow descent through the lower stratosphere and the TTL. Two flights of this type were completed on 5 and 23 August.

– *Anvil and Cirrus* was intended to sample cloud tops and turrets and document possible impact of lightning and convective overshoot. The payload was made of remote sensing instruments: the micro-LIDAR, SAOZ-H_2O, IR-radiometer, HV-AIRS and lightning optical detectors. The objective was to fly directly next or above thunderstorms, at about 22 km and then to descent very slowly accross the tropopause. A successful flight in the vicinity of a storm area was achieved on 7 August.

– Finally, *Chemistry* was to study NO_x production by lightning, bromine chemistry (CH_3Br and BrO) and radiation. The payload associated a SAOZ, a SAOZ-BrO, micro-DIRAC and NILUCUBE. The plan was to fly in the afternoon downwind of a MCS for daytime in situ measurements during ascent up to 28–30 km followed by remote westward cloud free observations at sunset from float altitude. Two flights were achieved, on 10 and 19 August.

The average duration of the flights was of 3–4 h with landings 100–200 km west of Niamey. Payload were recovered typically after 2–3 days, often delayed by flooding in the region, and their refurbishment required 2 to 3 more days. The list of the balloon payloads and data availability for these flights is provided in Table 2. Each flight track is shown on Fig. 12 superimposed to MSG 10.8 μm brightness temperature images high cloud tops (T<65°C), which are a proxy for convective activity, are in coded in orange.

Twenty-nine sondes were flown between 26 July and 25 August all carrying a Vaisala RS92 PTU and an ozone sensor, 9 of them a BKS sonde, and 6 both a BKS and a FLASH hygrometer. When possible the BKS or BKS/FLASH flights were conducted in conjunction with the balloon flights described above. The list of soundings is given in Table 3.

ACPD
9, 19713–19781, 2009

Here is a brief report of balloon and sonde flights carried out each day, data availability and main features observed during each of them.

4.2.1 31 July (Julian day 212) OPC and CN counter and Ice and Aerosols #1

The balloon was launched at 08:30 UTC before the arrival of an MCS (gust front and squall line at 09:20, lightning at 24 flashes per minute due south, cloud tops around 13 km). It ended at 11:00. Particles and CN measurements during ascent to 32 km and fast parachute descent show a thick cloud of particles, radius $\leq 1\,\mu$m between 13–17.5 km and further particles of up to 2 μm radius up to 24 km during the ascent. The balloon went through thick clouds during the ascent. Subsequent analysis coupled with additional flights suggests that the measurements were contaminated in the UTLS by outgassing of water vapour from the gondola on both ascent and descent.

The *Ice and Aerosols* flight was launched at 17:23 and ended at 19:26 UTC. No data could be recovered for OPC, Micro-Dirac and micro-SDLA due to a rough launch. LABS only acquired backscatter ratio and depolarization data up to 22 km during ascent and descent.

4.2.2 2 August (Julian day 214) BKS /O_3 sonde

The flight was launched at 18:52 UTC. Cloud layers from 15 to CPT at 17 km with high colour indices (around 15) indicating the presence of ice particles, and a layer of particles between 19–21.5 km with low colour indices, indicating small liquid sulphate aerosols, were observed. This high altitude layer, present in all BKS soundings, was later identified to be volcanic aerosols from the eruption of the Soufriere Hills volcano in Monserrat Island in the Caribbean on 20 May 2006 (Vernier et al., 2009).

4.2.3 3 August (Julian Day 215) BKS/FLASH/O_3 sonde

It was launched at 18:38 UTC. Thick clouds between 11–13 km and 14–16 km and the volcanic plume between 19–21.5 km were observed. FLASH reported 5 ppmv at the

ACPD
9, 19713–19781, 2009

cold point tropopause, a 4.5 ppmv minimum around 20 km and an almost constant 5.5 ppmv mixing ratio above.

4.2.4 5 August (Julian Day 217) Water Vapour #1 and BKS/FLASH/O_3 sonde

The balloon was launched after sunset at 18:40 UTC in local "suppressed convection" situation with a MCS 600–800 km upstream in the NE over the Aïr mountains and another very large one 1000 km East, over SW Chad. Satellite observations as well as mesoscale modelling studies show that the Aïr MCS was generated orographically over Aïr and has induced overshoots up to 18.3 km (Liu et al., 2009). CH_4 is showing constant 1.8 ppmv MR up to the tropopause at 16.5 km, decreasing above at an average rate of 0.11 ppmv/km and enriched layers around 7.5 and 19 km. H_2O is displaying a local minimum at 16 km surmounted by relatively moist layers at 17–17.5 km and 17.9 km and the hygropause at 18.1 km. However, although the fine structures are qualitatively consistent with FLASH observations on the same day, micro-SDLA shows a still unexplained dry bias.

As for the LABS measurements, noticeable are the non-depolarizing and thus liquid volcanic particles layer several hundreds metres thick at 20 km seen during both ascent and descent, an extremely thin layer of few tens of metres of depolarizing particles at 13 km on descent corresponding with a local water vapour minimum and a two kilometre thick layer of depolarizing particles at 9–11 km during descent. Launched 12 min later at 18:52 UTC, the BKS/FLASH/Ozone sonde showed a cold point tropopause at 16.7 km with 6.2 ppmv H_2O surmounted by hydrated layers of 8 ppmv at 17 km that Khaykin et al. (2009) have linked to lower stratosphere hydration by overshooting convection over Chad, further transported to the Niamey area. The role of the Chad overshooting system is confirmed by the Cloud Resolving Model simulation of Liu et al. (2009). Another hydrated layer is shown at 17.8 km, and a minimum of 4.25 ppmv at 19 km., whilst the BKS was showing particles slightly below 17 km and above 17.5 km and the volcanic plume at 20 km.

4.2.5 7 August (Julian Day 219) Anvil and Cirrus #1 and BKS/FLASH/O_3 sonde

The balloon was launched at 16:45 UTC before an intense MCS travelling from the East (tops at 19 km seen by the radar 2 h before, lightning 18 flashes/min), which caused heavy rain as the balloon was already in flight. After a 40 min float at 22.5 km, the balloon descended slowly down to 18.7 km at 20:10 UTC. At the time of the launch, a large convective area was located 100 km S-SE and a MCS 100 km west. Another active cell developed 200 km to the west, which was over-flown by the balloon at the end of the flight. The available data are SAOZ O_3 and NO_2 profiles (70–80 ppt NO_2 in troposphere, increase above CPT (250 ppt at 20 km); SAOZ H_2O (7 ppmv at CPT, minimum 4 ppmv at 20 km very consistent with the FLASH measurements on the same day); SAOZ aerosol wavelength dependent extinction at 20 km (particles of 0.4 μm effective radius); micro-lidar clouds at 12–13 km and 14.5–15.5 km and particles layers at 18.2, 19.8 and 21 km during ascent, thin cirrus at 15 km after sunset, a permanent 1 km thick cloud layer at 14 km during the night dropping slowly to 13 km and higher cloud tops at 14 km (also seen by the radar) at the end of the flight confirmed by a drop of brightness temperature in the global IR radiometer. The vertical electric field of ~2.5 V/m at 22.5 km ceiling altitude was directed downward as expected in quite fair weather with the closest active MCS a few tens of kilometres south. The positive and negative conductivities at 22.5 km were respectively ~2.10–13 S/m and 3.10–13 S/m, about 2–3 times less but within the range of previous measurements at this latitude. Most unexpected was the observation of small scale features in the DC electric field during ascent indicative of the crossing of electrically charged structures with typical dimensions of 30 to 50 m between about 16.8 and 19 km altitude. In addition, the AC channel recorded several hundred impulsive signals during the flight, originating from the EM waves emitted by lightning a few hundred kilometres away. Finally at the end of the flight, after sunset, the optical detectors detected a large number of flashes from the near-by active MCS and the triggered DC and AC electric field disturbances, as reported in Berthelier et al. (2009) and Berthelier et al. (2009). The BKS/FLASH/ O_3

ACPD
9, 19713–19781, 2009

sonde was launched at 18:38 UTC, finding a CPT at 17 km after crossing a thick cloud up to 14 km, above which a number of thin particles layers were observed between 14–18 km. FLASH was reporting 6 ppmv H_2O from 16.5 to 17.5 km, and a hygropause of 4.5 ppmv at 20 km.

4.2.6 9 August (Julian Day 221) BKS/FLASH/O_3 sonde

Launched at 18:39 UTC, it showed a a CPT of −78°C at 17 km. No cloud or ice particles were observed during this flight but the volcanic plume at 20 km.

4.2.7 10 August (Julian Day 222) Chemistry #1

The balloon was launched at 16:42 UTC reaching float altitude at 28.8 km for 44 min followed by descent after sunset for 39 min. The radar could see a MCS at 200–300 km in the SE topping at 15 km, and convective cells on the west organising in squall line on the west, flown over by the balloon. The CPT of −78°C was crossed at ∼17.3 km. The data available are those of SAOZ O_3 and NO_2, the last showing a peak of 140 ppt at 11–13 km on both ascent and sunset, likely due to lightning, and SAOZ-BrO showing low BrO until 17 km (≤3 ppt,) increasing rapidly above (20 ppt at 25 km). The NILU-CUBE operated successfully throughout the full flight with UV radiation measurements at 1 s intervals. However since it was lost later in the campaign (on 19 August), post-calibration of the data was then not possible, which was assessed instead by comparison with model simulations, adding more uncertainty to the resulting actinic fluxes and photolysis rates (Engelsen et al., 2009).

4.2.8 12 August (Julian Day 226) BKS/O_3 sonde

Launched at 18:38 UTC it reached the CPT of −78°C at 17 km after crossing depolarizing clouds between 13.3–14.5 km. Some small particles were reported between 15–17 km followed by the volcanic plume at 20 km.

ACPD
9, 19713–19781, 2009

4.2.9 14 August (Julian Day 226) BKS/FLASH/O_3 sonde

Launched at 18:46 UTC, it crossed a CPT of −81°C at 16.5 km. The BKS reported thick cloud layers at 9–13 km, 13.5–15 km and 15–17 km, followed by thin particles layers between 17–18 km, and the volcanic plume above. The water vapour was 6 ppmv at the CPT, followed by a 7.5 ppmv 500 m thick layer immediately above, and another increase at 18.2 km. The hygropause was at about 20 km.

4.2.10 17 August 2006 (Julian Day 229) Ice and aerosol #2

Launched at 11:45 UTC it ascended to ∼22 km followed by 30 min at ceiling and a slow descent to 14.5 km in 1.5 h. There was no convective activity in the proximity of the balloon but a large MCS over eastern Niger, 800 km east. The CPT of −78°C was observed at 16.5 km. The data available are the OPC size distribution of the volcanic aerosol between 19–20 km (2 cm^{-3} of $r \geq 0.15\,\mu m$, 0.5 cm^{-3} of $r \geq 0.25\,\mu m$, 0.08 cm^{-3}, $r \geq 0.5\,\mu m$); the LABS backscatter ratio displaying a cloud layer at 8–9 km, also observed by OPC, a high depolarizing layers at 16.5 km, and the non depolarizing volcanic plume at 20 km. Finally the Micro-DIRAC got several CH_3CCl and CCl_4 vmr samplings during ascent up to 22 km.

4.2.11 19 August (Julian Day 231) Chemistry #2

Launched at 16:45 UTC it reached the float level at 29.2 km at 18:00 and was cut down after sunset. No local convective activity was present but a strong MCS 100–200 km upwind on the east. The CPT was at −74°C at 17 km. SAOZ observed a thick NO_2 layer of up to 350 ppt between 13 and 17 km during the ascent, absent later at 400 km distance in the W-NW at sunset. SAOZ-BrO showed less than 3 ppt up to 18.5 km and a rapid increase above 20 km to 20 ppt at 25 km. Unfortunately no data are available from the NILU-CUBE instrument that we failed to recover.

ACPD
9, 19713–19781, 2009

4.2.12 21 August (Julian Day 235) BKS/FLASH/O_3 sonde

Launched at 21:52 UTC with a 400 km size MCS nearby on the East it crossed a CPT of −82°C at 16.5 km. BKS observed a thick cloud from 11 to 16.8 km, several thin layers of particles up to 18.5 km an the volcanic plume above. FLASH reported a water vapour mixing ratio of 5 ppmv at the CPT, a 6.5 ppmv layer 1 km above and the hygropause at 20 km.

4.2.13 23 August (Julian Day 235) Water vapour #2 and BKS/FLASH/O_3 sonde

Water vapour #2 was launched at 18:15 UTC reaching a ceiling altitude of 24.7 km followed by a slow descent to 14 km in 1 h20 min. This flight took place after a two day period of intense convection over Niamey area. The MSG images were showing an MCS immediately north, local convection on the west of the Niger river and other MCS along the Nigeria border. Before launch, the MIT radar was reporting convective cells reaching 18 km.

The temperature profile was singular showing a marked LRT of −76°C at 15 km followed by a CPT of −80°C at 17 km. Methane shows a slightly increasing mixing ratio of about 180 ppmv until 15 km, above which it decreases by 0.105 ppmv/km with some enriched layers at 18 km and 20 km. Though the micro-SDLA experienced similar dry bias compared to FLASH as in its first flight, water vapour displays a minimum at the LRT followed immediately above by a 1 km thick hydrated layer and another thin enriched layer of smaller amplitude just below 18 km. The hygropause was found at 20 km. On the same flight, LABS reported thick clouds between 12 km and the tropopause both on ascent and descent, and a thin layer of depolarizing particles on ascent at 19 km.

The BKS /FLASH/O_3 sonde was launched 53 min later at 19:07 UTC. A CPT of −78°C was observed at 15.5 km. The backscatter sonde sampled a thick cloud between 13–16 km on both ascent and descent and a 1 km thick particles layer during descent around 18 km with high colour indices (15–20) but low depolarization. FLASH

ACPD
9, 19713–19781, 2009

measured a 6 ppmv minimum at the tropopause, followed by a 13 ppmv 1 km thick layer immediately above, and another 7 ppmv layer at 18 km qualitatively very similar to those reported by micro-SDLA. More details on the FLASH and BKS measurements can be found in (Khaykin et al., 2009).

4.2.14 Ozonesondes

Almost daily ozonesondes were performed between 26 July and 25 August, some of them combined with the flights decribed previously. These ozone profiles are displayed in Fig. 13: they show steady increasing values from 0.03 ppmv at the surface to 0.1 ppmv around 15 km a little below the CPT (Reeves et al., 2009). Above 15 km the ozone mixing ratios increase rapidly throughout the TTL. The profiles show remarkably small day to day changes except in the planetary boundary layer and in the upper troposphere where lower ozone was observed on 14 August and higher on 2 and 23 August.

5 Scientific highlights

Overall the stratospheric aircraft, balloon and sonde data collected during the campaign produced a large amount of observations on the impact of deep convective systems and large-scale transport on the lower stratosphere. Among most interesting results, aside from the observation of a large impact of convection and surface heating on the thermal structure of the lower stratosphere shown by the diurnal cycle of temperature, are the water observations in the TTL and in the lower stratosphere. On average, water vapour measurements present the typical profile of the Northern Hemisphere summer: a relatively wet (6 ppmv) cold point with a slowly decreasing mixing ratio above, to approximately 4.2–4.5 ppmv at the hygropause at about 19–20 km (68–58 hPa, 440–470 K) (Khaykin et al., 2009; Schiller et al., 2009). The balloon profiles over Niamey and those of the M-55 Geophysica further west are very consistent, both in qualitative and

ACPD
9, 19713–19781, 2009

quantitative terms. Below the cold point, the bulk of convective outflow strongly moistens the TTL and the observations of high specific humidity are frequently accompanied by high relative humidity, sometimes super-saturation, and cloud particles. Above the cold point, a noticeable difference between our measurements and the low-vertical-resolution, smooth, satellite observations reported previously, is the presence of highly structured layers of enhanced water vapour. Though observed in sub-saturated air, few observations also show particles at the same levels. All water vapour layers have been observed either close to deep convective events or could be traced by back trajectory calculations to regions with likely overshoots into the stratosphere (Khaykin et al., 2009; Fierli et al., 2009). These observations in particular those reported several hours downwind a MCS occurrence, are clear indication that deep convection has the potential to moisten the TTL above the cold point irreversibly, as also shown by the SCOUT-O_3 M-55 measurements in Darwin (Corti et al., 2008). Injection of tropospheric air in the layers of enhanced water vapour is apparent also in the coincident ozone profile measured on the same balloon (Khaykin et al., 2009). However, the importance of the contribution of these local events to the stratospheric water budget on a global scale is still uncertain.

A very new observation provided by the HV-AIRS probe is the observation that the ice crystals injected in the stratosphere are electrically charged which may have consequences on their vertical motion as well as on their lifetime, processes currently under further examination (Berthelier et al., 2009). The average level of main convective outflow was located between 350 and 360 K (one day reaching 370 K) (Homan et al., 2009; Fierli et al., 2009; Law et al., 2009) or 14–15 km, indicating the level of the mean outflow: IRIS water isotope profiles of 7 August show slight deviations from Rayleigh-like gradual depletion between 330 and 370 K that is possibly indicative of convective ice-lofting to altitudes below the cold point (Iannone et al., 2009). In general, there is less compelling evidence of irreversible mixing after overshooting of convective air from tracer measurement than from water measurements. The fact that overshooting has no large impact on vertical profile of tracers (Homan et al., 2009; Fierli et al., 2009; Law

ACPD
9, 19713–19781, 2009

et al., 2009) is probably due to the different sensitivities of tracer and water substance profiles to vertical mixing, water being the most sensitive while long lived tracers are less sensitive. Moreover it has to be stressed that no fresh convection appears to have been measured by the M55, so that tracer measurements from the Geophysica may not have picked up the signal of fresh convective injection.

Stratospheric trace gas correlations and profiles showed that the observed region was mainly outside the so-called isolated tropical pipe (Plumb, 1996) – only the last M55 flight toward the equator was able to reach into it. Air mixing in from the extratropical stratosphere became discernible in the LS (Homan et al., 2009; Law et al., 2009) while no evidence was found for isentropic in-mixing from extratropical stratosphere in the TTL below the tropical tropopause (Homan et al., 2009). Cross-hemispheric tropical transport in the middle and upper troposphere was also reported (Real et al., 2009).

In general, the African TTL in August appeared to be wetter and warmer than the one observed in November in Darwin, with much higher CN and O_3 in lower stratosphere. Backtrajectory and RDF analysis (Law et al., 2009) showed how the African Lower stratosphere was influenced by an influx from north-east Asia, probably in connection with Asian monsoon anticyclone activity (Schiller et al., 2009).

A permanent particle layer between 19–20 km detected by balloon, sondes and aircraft of small (30 cm^3 $\leq$0.15 μm OPC, 40 cm^3 COPAS), not depolarizing and thus liquid (LABS) particles, present at all longitude between 10–20° S (CALIPSO) (Homan et al., 2009), following the eruption of La Soufriere Hills volcano in Monserrat Island in the Caribbean on 20 May 2006, whose SO_2 cloud was observed during one week after the eruption by the AURA-OMI satellite (Carn et al., 2007; Prata et al., 2007). Particle number density showed a large variability in the troposphere, with events of fresh particle nucleation frequently observed, probaby due to MCS activity providing favourable conditions for particle formation. The stratospheric number density profile was compact, with the total particle number and its non-volatile fraction respectively increasing and decreasing upward (Borrmann et al., 2009).

Large reactive nitrogen (NO_y) containing particles were observed on 8 August 2006 by instruments onboard the high altitude research aircraft M55-Geophysica near and below the tropical tropopause. The particles, most likely NAT, had dilute concentrations below 10^{-4} cm^{-3} and diameters less than 6 μm. The NAT particle layer extended between 15.1 and 17.5 km over large areas. Satellite observations suggest that the NAT particles could have nucleated on ice fed by convective activity. The in-situ detection of NAT particles combined with global model simulations indicate the potential for a tropical tropopause NAT particle belt (Voigt et al., 2008).

These valuable observations contribute to build global picture of the tropical LS and TTL and are of even more value since they came from Sahelian Africa, a region heavily under sampled in terms of atmospheric observations.

6 Conclusions

A tropical stratospheric aircraft, balloon and sonde campaign has been successfully conducted in West Africa during the peak of the 2006 monsoon season, in the framework of the observational activities of the EU funded projects AMMA and SCOUT-O_3. The campaign aimed: to study the effects of deep convection on trace gases, aerosols and water vapour distributions; to characterize the chemical composition and the transport mechanisms in the UTLS over West Africa; and to validate the CALIOP products in terms of observed aerosol and cirrus properties.

Successful measurements of water vapour, ozone, particles and trace gases were accomplished from different instruments on different platforms, providing a comprehensive picture of the TTL and lower stratosphere of the region.

This paper has provided the general overview of the campaign in terms of observational activities and meteorological context and has illustrated the main highlights of the experimental results. A detailed analysis of the measurements is presented in other focused papers.

ACPD
9, 19713–19781, 2009

Acknowledgements. The balloon campaign was supported by the EC Integrated Project SCOUT-O_3 (505390-GOCE-CT-2004).

The M55-Geophysica campaign was supported by the EEIG-Geophysica Consortium, CNRS-INSU, EC Integrated Projects AMMA-EU (Contract Number 004089-2), SCOUT-O_3 and CNES.

The deployment of IRIS and WAS was partially supported by the European Fleet for Airborne Research project (EUFAR) (EC-FP6 Contract Number 506514).

The OPC measurements were partly funded by the US National Science Foundation.

The DLR Falcon F-20 campaign was funded through AMMA-EU and DLR.

The radiosoundings in Niamey were funded by AMMA-EU and the ARM program (US DoE).

We would like to thank all the scientists, aircraft operators as well as local scientists and representatives in Burkina Faso for their help and support during the planning and execution of the Ouagadougou campaign. Stefano Balestri and Ana Alfaro Martinez (ERS) are gratefully acknowledged for their operations in Verona and Ouagadougou. Kare Edvardsen and Tron Danielsen (NILU), Sergey Kaikhin (CAO, Russia) and Pierre Francois (Service d'Aeronomie) assisted in the preparation and operation of the NILU-CUBE.

We also acknowledge support from the AMMA Operations Centre in Niamey, Niger.

Based on a French initiative, AMMA was built by an international scientific group and is currently funded by a large number of agencies, especially from France, the United Kingdom, the United States, and Africa. It has been a beneficiary of a major financial contribution from the European Community Sixth Framework Programme (AMMA-EU). Detailed information on scientific coordination and funding is available on the AMMA International website at www.amma-international.org.

References

Alcala, C. M., and Dessler, A. E.: Observations of deep convection in the tropics using the Tropical Rainfall Measuring Mission (TRMM) precipitation radar, J. Geophys. Res., 107(D24), 4792, doi:10.1029/2002/D002457, 2002. 19717

Berthelier, J. J., Simões, F., Pommereau, J. P., and Vernier, J. P.: Observation of stratospheric charged cirrus and their relation with water transport in the tropical UTLS, in preparation, 2009. 19746, 19751

Berthelier, J. J., Simões, F., and Pommereau, J. P.: Balloon borne DC and AC Electric Field measurements in the vicinity of tropical convective clouds, Workshop on Coupling of Thunderstorms and Lightning Discharges to Near-Earth Space, Corte, Corsica, June, 2008.

Berthelier, J. J., Simões, F., and Pommereau, J. P.: Balloon observations of impulse variations of the atmospheric electric field associated with lightning from a tropical MCS, in preparation, 2009. 19746

Borrmann, S., Luo, B., and Mishchenko, M.: The application of the T-matrix method to the measurement of aspherical particles with forward scattering optical particle counters, J. Aerosol Sci., 31, 789–799, 2000. 19728

Borrmann, S., Kunkel, D., Weigel, R., Minikin, A., Deshler, T., Wilson, J. C., Curtius, J., Sitnikov, N. M., Ulanovsky, A., Schiller, C., Ravegnani, F., Law, K. S., and Cairo, F.: Aerosols in the tropical and subtropical UT/LS: In-situ measurements of ultrafine particle abundance and volatility, in preparation, 2009. 19752

Brunner, D., Siegmund, P., May, P. T., Chappel, L., Schiller, C., Müller, R., Peter, T., Fueglistaler, S., MacKenzie, A. R., Fix, A., Schlager, H., Allen, G., Fjaeraa, A. M., Streibel, M., and Harris, N. R. P.: The SCOUT-O_3 Darwin Aircraft Campaign: rationale and meteorology, Atmos. Chem. Phys., 9, 93–117, 2009, http://www.atmos-chem-phys.net/9/93/2009/. 19719

Buontempo, C., Cairo, F., Di Donfrancesco, G., Morbidini, R., Viterbini, M., and Adriani, A. : Optical measurements of atmospheic particles from airborne platform: in-situ and remote sensing instruments for balloons and aircrafts, Ann. Geophys.-Italy, 49, 57–64, 2006. 19725

Cairo, F., Adriani, A., Viterbini, M., Di Donfrancesco, G., Mitev, V., Matthey, R., Bastiano, M., Redaelli, G., Dragani, R., Ferretti, R., Rizi, V., Paolucci, T., Bernardini, L., Cacciani, M., Pace, G., and Fiocco, G.: Polar stratospheric clouds observed during the Airborne Polar ExperimentGeophysica Aircraft in Antarctica (APE-GAIA) campaign, J. Geophys. Res., 109,

D07204, doi:10.1029/2003JD003930, 2004. 19725
Carn, S. A., Krotkov, N. A., Yang, K., Hoff, R. M., Prata, A. J., Krueger, A. J., Loughlin, S. C., and Levelt, P. F.: Extended observations of volcanic SO_2 and sulfate aerosol in the stratosphere, Atmos. Chem. Phys. Discuss., 7, 2857–2871, 2007, http://www.atmos-chem-phys-discuss.net/7/2857/2007/. 19752
Chaboureau, J.-P., Cammas, J.-P., Duron, J., Mascart, P. J., Sitnikov, N. M., and Voessing, H.-J.: A numerical study of tropical cross-tropopause transport by convective overshoots, Atmos. Chem. Phys., 7, 1731–1740, 2007, http://www.atmos-chem-phys.net/7/1731/2007/. 19717, 19718
Corti, T., Luo, B. P., Peter, P., Vömel, H., and Fu, Q.: Mean radiative energy balance and vertical mass fluxes in the equatorial upper troposphere and lower stratosphere, Geophys. Res. Lett., 32, L06802, doi:10.1029/2004GL021889, 2005.
Corti, T., Luo, B. P., de Reus, M., Brunner, D., Cairo, F., Mahoney, M. J., Martucci, G., Matthey, R., Mitev, V., dos Santos, F. H., Schiller, C., Shur, G., Sitnikov, N. M., Spelten, N., Vossing, H. J., Borrmann, S., and Peter, T.: Unprecedented evidence for overshooting convection hydrating the tropical stratosphere, Geophys. Res. Lett., 35, L10810, doi :10.1029/2008GL033641, 2008. 19717, 19751
Curtius, J., Weigel, R., Vössing, H.-J., Wernli, H., Werner, A., Volk, C.-M., Konopka, P., Krebsbach, M., Schiller, C., Roiger, A., Schlager, H., Dreiling, V., and Borrmann, S.: Observations of meteoric material and implications for aerosol nucleation in the winter Arctic lower stratosphere derived from in situ particle measurements, Atmos. Chem. Phys., 5, 3053–3069, 2005, http://www.atmos-chem-phys.net/5/3053/2005/. 19728
D'Amato, F., Mazzinghi, P., and Castagnoli, F: Methane analyzer based on TDL's for measurements in the lower stratosphere: design and laboratory tests, Appl. Phys. B75, 195–202, 2002. 19726
Danielsen, E. F.: A dehydration mechanism for the stratosphere, Geophys. Res. Lett., 9(6), 605–608, 1982. 19717
Danielsen, E. F.: In situ evidence of rapid, vertical, irreversible transport of lower tropospheric air into the lower stratosphere by convective cloud turrets and by large scale up welling in tropical cyclones, J. Geophys. Res., 98, 8665–8681, 1993. 19717, 19724
de Reus, M., Borrmann, S., Heymsfield, A. J., Weigel, R., Schiller, C., Mitev, V., Frey, W., Kunkel, D., Kürten, A., Curtius, J., Sitnikov, N. M., Ulanovsky, A., and Ravegnani, F.: Evidence for

ice particles in the tropical stratosphere from in-situ measurements, Atmos. Chem. Phys. Discuss., 8, 19313–19355, 2008, http://www.atmos-chem-phys-discuss.net/8/19313/2008/. 19728

Deshler, T., Hervig, M. E., Hofmann, D. J., Rosen, J. M., and Liley, J. B.: Thirty years of in situ stratospheric aerosol size distribution measurements from Laramie, Wyoming (41 N), using balloon-borne instruments, J. Geophys. Res., 108(D5), 4167, doi:10.1029/2002JD002514, 2003. 19731

Deshler, T., Anderson-Sprecher, R., Jäger, H., Barnes, J., Hofmann, D. J., Clemesha, B., Simonich, D., Osborn, M., Grainger, R. G., and Godin-Beekmann, S.: Trends in the nonvolcanic component of stratospheric aerosol over the period 1971–2004, J. Geophys. Res., 111, D01201, doi:10.1029/2005JD006089, 2006. 19732

Di Donfrancesco, G., Cairo, F., Buontempo, C., Adriani, A., Viterbini, M., Snels, M., Morbidini, R., Piccolo, F., Cardillo, F., Pommereau, J. P., and Garnier, A.: Balloonborne lidar for cloud physics studies, Appl. Optics, 45, pp 1–8, 2006. 19731

Durry, G., Amarouche, N., Zéninari, V., Parvitte, B., Lebarbu, T., and Ovarlez, J.: In situ sensing of the middle atmosphere with balloonborne near-infrared laser diodes, Spectrochim. Acta A, 60(4), 3371–3379, 2004. 19730

Engelsen, O., Danielsen, T., Kift, R., Webb, and A. R.: Analysis and reconstructions of measured vertical UV radiation profiles during campaigns in Thessaloniki, Greece and Niamey, Niger, in preparation, 2009.

Ern, M., Preusse, P., Krebsbach, M., Mlynczak, M. G., and Russell III, J. M.: Equatorial wave analysis from SABER and ECMWF temperatures, Atmos. Chem. Phys., 8, 845–869, 2008, http://www.atmos-chem-phys.net/8/845/2008/. 19722

Fierli, F., Orlandi, E., Cairo, F., Law, K. S., et al. : Characterization of the convective outflow in the UTLS region during the AMMA campaign: impact in the upper troposphere and mesoscale simulations, in preparation, 2009. 19751

Fischer, H., Birk, M., Blom, C., Carli, B., Carlotti, M., von Clarmann, T., Delbouille, L., Dudhia, A., Ehhalt, D., Endemann, M., Flaud, J. M., Gessner, R., Kleinert, A., Koopman, R., Langen, J., López-Puertas, M., Mosner, P., Nett, H., Oelhaf, H., Perron, G., Remedios, J., Ridolfi, M., Stiller, G., and Zander, R.: MIPAS: an instrument for atmospheric and climate research, Atmos. Chem. Phys., 8, 2151–2188, 2008, http://www.atmos-chem-phys.net/8/2151/2008/. 19727

Folkins, I., Loewenstein, M., Podolske, J., Oltmans, S. J., and Profitt, M.: A barrier to vertical

mixing at 14 km in the tropics: Evidence from ozonesondes and aircraft measurements, J. Geophys. Res., 104, 22095–22102, 1999.
Folkins, I., Braun, C., Thompson, A. M., and Whitte, J.: Tropical ozone as an indicator of deep convection, J. Geophys. Res., 107(D13), 4184, doi:10.129/2001JD001178, 2002.
Folkins, I., Bernath, P., Boone, C., Lesins, G., Livesey, N., Thompson, A. M., Walker, K., and Witte, J. C.: Seasonal cycles of O_3, CO and convective outflow at the tropical tropopause, Geophys. Res. Lett., 33, L16802, doi:10.1029/2006GL026602, 2006.
Franz, P. and R—"ockmann, T.: High-precision isotope measurements of $H_2$16O, $H_2$17O, $H_2$18O, and the Δ17O-anomaly of water vapor in the southern lowermost stratosphere, Atmos. Chem. Phys., 5, 2949–2959, 2005 19727
Fueglistaler, S., Dessler, A. E., Dunkerton, T. J., Folkins, I., Fu, Q., and Mote, P. W. : The tropical tropopause layer, Rev. Geophys., 47, RG1004, doi:10.1029/2008RG000267, 2009. 19717
Gettelman, A., Salby, M. L., and Sassi, F.: The distribution and influence of convection in the tropical tropopause region, J. Geophys. Res., 107(D10), doi:10.1029/2001JD001048, 2002. 19717
Gettelman, A., Kinnison, D. E., Dunkerton, T. J., and Brasseur, G. P.: Impact of monsoon circulations on the upper troposphere and lower stratosphere, J. Geophys. Res., 109, D22101, doi:10.1029/2004JD004878, 2004. 19717
Gostlow, B., Robinson, A. D., Pyle, J. A., Harris, N. R. P., and OBrien, L.: Micro-DIRAC: An Autonomous Instrument for Halocarbon Measurements, submitted to Atmospheric Measurement Techniques, 2009. 19730
Grosvenor, D. P., Choularton, T. W., Coe, H., and Held, G.: A study of the effect of overshooting deep convection on the water content of the TTL and lower stratosphere from Cloud Resolving Model simulations, Atmos. Chem. Phys., 7, 4977–5002, 2007, http://www.atmos-chem-phys.net/7/4977/2007/. 19718
Hall, N. M. J. and Peyrillé, P.: Dynamics of the West African monsoon, J. Phys. IV France, 139, 81–99, 2006. 19720
Highwood, E. J. and Hoskins, B. J.: The tropical tropopause, Q. J. Roy. Meteorol. Soc., 124, 1579–1604, 1998. 19717
Hoffmann, L., Weigel, K., Spang, R., Schroeder, S., Arndt, K., Lehmann, C., Kaufmann, M., Ern, M., Preusse, P., Stroh, F., and Riese, M.: CRISTA-NF measurements of water vapor during the SCOUT-O_3 Tropical Aircraft Campaign, Adv. Space Res., 43, 74–81,

doi:10.1016/j.asr.2008.03.018, 2009. 19727
Homan, C. D., Volk, C. M., Kuhn, A. C., Werner, A., Baehr, J., Viciani, S., Ulanovski, A., and Ravegnani, F.: Tracer measurements in the tropical tropopause layer during the SCOUT-AMMA aircraft campaign, in preparation, 2009. 19751, 19752
Huntrieser, H., Schumann, U., Schlager, H., Höller, H., Giez, A., Betz, H.-D., Brunner, D., Forster, C., Pinto Jr., O., and Calheiros, R.: Lightning activity in Brazilian thunderstorms during TROCCINOX: implications for NO_x production, Atmos. Chem. Phys., 8, 921–953, 2008, http://www.atmos-chem-phys.net/8/921/2008/. 19719
Iannone, R. Q., Kassi, S., Jost, H.-J., Chenevier, M., Romanini, D., Meijer, H. A. J., Dhaniyala, S., Snels, M., and Kerstel E. R. T.: Development and airborne operation of a compact water isotope ratio infrared spectrometer, Isotopes in Environmental and Health Studies, 1, 99999, doi:10.1080/10256010903172715, 2009. 19751
Immler, F., Krüger, K., Fujiwara, M., Verver, G., Rex, M., and Schrems, O.: Correlation between equatorial Kelvin waves and the occurrence of extremely thin ice clouds at the tropical tropopause, Atmos. Chem. Phys., 8, 4019–4026, 2008, http://www.atmos-chem-phys.net/8/4019/2008/.
Janicot, S., Thorncroft, C. D., Ali, A., Asencio, N., Berry, G., Bock, O., Bourles, B., Caniaux, G., Chauvin, F., Deme, A., Kergoat, L., Lafore, J.-P., Lavaysse, C., Lebel, T., Marticorena, B., Mounier, F., Nedelec, P., Redelsperger, J.-L., Ravegnani, F., Reeves, C. E., Roca, R., de Rosnay, P., Schlager, H., Sultan, B., Tomasini, M., Ulanovsky, A., and ACMAD forecasters team: Large-scale overview of the summer monsoon over West Africa during the AMMA field experiment in 2006, Ann. Geophys., 26, 2569–2595, 2008, http://www.ann-geophys.net/26/2569/2008/. 19720, 19722
Kaiser, J., Engel, A., Borchers, R., and Röckmann, T.: Probing stratospheric transport and chemistry with new balloon and aircraft observations of the meridional and vertical N_2O isotope distribution, Atmos. Chem. Phys., 6, 3535–3556, 2006, http://www.atmos-chem-phys.net/6/3535/2006/. 19727
Kerstel, E. R. T., Iannone, R. Q., Chenevier, M., Kassi, S., Jost, H.-J., and Romanini, D.: A water isotope (2H, 17O, and 18O) spectrometer based on optical-feedback cavity enhanced absorption for in-situ airborne applications, Appl. Phys. B, 85(2–3), 397–406, 2006. 19726
Khaykin, S., Pommereau, J.-P., Korshunov, L., Yushkov, V., Nielsen, J., Larsen, N., Christensen, T., Garnier, A., Lukyanov, A., and Williams, E.: Hydration of the lower stratosphere by ice

crystal geysers over land convective systems, Atmos. Chem. Phys., 9, 2275–2287, 2009, http://www.atmos-chem-phys.net/9/2275/2009/. 19745, 19750, 19751

Kylling, A., Danielsen, T., Blumthaler, M., Schreder, J., and Johnsen, B.: Twilight tropospheric and stratospheric photodissociation rates derived from balloon borne radiation measurements, Atmos. Chem. Phys., 3, 377–385, 2003, http://www.atmos-chem-phys.net/3/377/2003/. 19732

Law, K. S.,Cairo, F., Fierli, F., Palazzi, E., Borrmann, S., Schlager, H., Streibel, M., Viciani, S., Ravegnani, F., Volk, C. M., Schiller, C., Some, L., et al.: Air mass origins influencing TTL chemical composition over West Africa during 2006 summer monsoon, in preparation, 2009. 19751, 19752

Kley, D. and Stone, E. J.: Measurements of water vapor in the stratosphere by photodissotiation with Ly-alpha (1216A) light, Rev. Sci. Instrum., 49, 661–697, 1978. 19733

Laube, J. C., Engel, A., Bönisch, H., Möbius, T., Sturges, W. T., Braß, M., and Röckmann, T.: Fractional release factors of long-lived halogenated substances in the tropical stratosphere, in preparation, 2009. 19727

Lebel, T., Parker, D. J., Flamant, C., Bourles, B., Marticorena, B., Mougin, E., Peugeot, C., Haywood, J. M., Polcher, J., Redelsperger, J.-L., and Thorncroft, C. D.: The AMMA field campaigns, Multiscale and multidisciplinary observations in the West African region, Q. J. Roy. Meteorol. Soc., in preparation, 2009. 19718, 19719

Liu, C. and Zipser, E. J.: Global distribution of convection penetrating the tropical tropopause, J. Geophys. Res. , 110, D23104, doi:10.1029/2005JD006063, 2005. 19717

Liu, X., Rivière, E. D., Marécal, V. , Durry, G., Hamdouni, H., and Arteta, J.: Water vapor budget associated to overshoots in the tropical stratosphere: mesoscale modeling study of 4–5 August 2006 during SCOUT-AMMA, in preparation, 2009. 19745

Marécal, V., Durry, G., Longo, K., Freitas, S., Rivière, E. D., and Pirre, M.: Mesoscale modelling of water vapour in the tropical UTLS: two case studies from the HIBISCUS campaign, Atmos. Chem. Phys., 7, 1471–1489, 2007, http://www.atmos-chem-phys.net/7/1471/2007/. 19730

Mote, P. W., Rosenlof, K. H., McIntyre, M. E., Carr, E. S., Gille, J C., Holton, J. R., Kinnersley, J. S., Pumphrey, H. C., Russell III, J. M., and Waters, J. W.: An atmospheric tape recorder: The imprint of tropical tropopause temperatures on stratospheric water vapor, J. Geophys. Res., 101, 3989–4006, 1996.

Morel, C. and Senesi, A.: A climatology of mesoscale convective systems over Europe using

satellite infrared imagery, I: Methodology, Q. J. Roy. Meteorol. Soc., 128(584), 1953–1971, 2002. 19719

Nielsen, J. K., Larsen, N., Cairo, F., Di Donfrancesco, G., Rosen, J. M., Durry, G., Held, G., and Pommereau, J. P.: Solid particles in the tropical lowest stratosphere, Atmos. Chem. Phys., 7, 685–695, 2007, http://www.atmos-chem-phys.net/7/685/2007/. 19717

Parker, D. J., Thorncroft, C. D., Burton, R. R., and Diongue-Niang, A.: Analysis of the African Easterly Jet, using aircraft observations from the JET2000 experiment, Q. J. Roy. Meteorol. Soc., 131, 1461–1482, 2005a. 19720

Parker, D. J., Burton, R. R., Diongue-Niang, A., Ellis, R. J., Felton, M., Taylor, C. M., Thorncroft, C. D., Bessemoulin, P., and Tompkins, A. M.: The diurnal cycle of the West African monsoon circulation, Q. J. Roy. Meteorol. Soc., 131, 2839–2860, 2005b. 19724

Parker, D. J., Fink, A., Janicot, S., Ngamini, J.-B., Douglas, M., Afiesimama, E., Agusti-Panareda, A., Beljaars, A., Dide, F., Diedhiou, A., Lebel, T., Polcher, J., Redelsperger, J.-L., Thorncroft, C., and Ato Wilson G.: 2008: The AMMA radiosonde program and its implications for the future of atmospheric monitoring over Africa, B. Am. Meteorol. Soc., 89, 1015–1027, 2009. 19723

Plumb, R. A.: A tropical pipe model of stratospheric transport, J. Geophys. Res., 101(D2), 3957–3972, 1996. 19752

Pommereau, J.-P., Garnier, A., Held, G., Gomes, A.-M., Goutail, F., Durry, G., Borchi, F., Hauchecorne, A., Montoux, N., Cocquerez, P., Letrenne, G., Vial, F., Hertzog, A., Legras, B., Pisso, I., Pyle, J. A., Harris, N. R. P., Jones, R. L., Robinson, A., Hansford, G., Eden, L., Gardiner, T., Swann, N., Knudsen, B., Larsen, N., Nielsen, J., Christensen, T., Cairo, F., Pirre, M., Marécal, V., Huret, N., Rivière, E., Coe, H., Grosvenor, D., Edvarsen, K., Di Donfrancesco, G., Ricaud, P., Berthelier, J.-J., Godefroy, M., Seran, E., Longo, K., and Freitas, S.: An overview of the HIBISCUS campaign, Atmos. Chem. Phys. Discuss., 7, 2389–2475, 2007, http://www.atmos-chem-phys-discuss.net/7/2389/2007/. 19717, 19719

Pommereau, J.-P. and Held, G.: Is there a stratospheric fountain?, Atmos. Chem. Phys. Discuss., 7, 8933–8950, 2007, http://www.atmos-chem-phys-discuss.net/7/8933/2007/. 19724

Pommereau, J.-P. and Piquard, J.: Ozone and nitrogen dioxide vertical distributions by UV-visible solar occultation from balloons, Geophys. Res. Lett., 21(13), 1227-1230, 1994. 19731

Popp, P. J., Marcy, T. P., Jensen, E. J., Kärcher, B., Fahey, D. W., Gao, R. S., Thompson, T. L., Rosenlof, K. H., Richard, E. C., Herman, R. L., Weinstock, E. M., Smith, J. B., May, R. D., Vömel, H., Wilson, J. C., Heymsfield, A. J., Mahoney, M. J., and Thompson, A. M.: The observation of nitric acid-containing particles in the tropical lower stratosphere, Atmos. Chem. Phys., 6, 601–611, 2006, http://www.atmos-chem-phys.net/6/601/2006/. 19739

Prata, A. J., Carn, S. A., Stohl, A., and Kerkmann, J.: Long range transport and fate of a stratospheric volcanic cloud from Soufrière Hills volcano, Montserrat, Atmos. Chem. Phys., 7, 5093–5103, 2007, http://www.atmos-chem-phys.net/7/5093/2007/. 19740, 19752

Pundt, I., Pommereau, J.-P., Chipperfield, M. P., Van Roozendael, M., and Goutail, F.: Climatology of the stratospheric BrO vertical distribution by balloon-borne UVvisible spectrometry, J. Geophys. Res., 107(D24), 4806, doi:10.1029/2002JD002230, 2002. 19731

Randel, W. J., Park, M., Wu, F., and Livesey, N. J.: A large annual cycle in ozone above the tropical tropopause linked to the Brewer-Dobson circulation, J. Atmos. Sci., 64, 4479–4488, doi:10.1175/2007JAS2409.1, 2007.

Real, E., Orlandi, E., Law, K. S., Fierli, F., Josset, D., Cairo, F., Schlager, H., Borrmann, S., Kunkel, D., Volk, M., McQuaid, J. B., Stewart, D. J., Lee, J., Lewis, A., Hopkins, J. R., Ravegnani, F., Ulanovski, A., and Liousse, C.: Cross-hemispheric transport of central African biomass burning pollutants: implications for downwind ozone production, Atmos. Chem. Phys. Discuss., 9, 17385–17427, 2009, http://www.atmos-chem-phys-discuss.net/9/17385/2009/. 19752

Redelsperger, J.-L., Thorncroft, C. D., Diedhiou, A., Lebel, T., Parker, D. J., and Polcher, J.: African Monsoon Multidisciplinary Analysis: An International Research Project and Field Campaign, B. Am. Meteorol. Soc., 87, 1739–1746, 2006. 19718

Reeves, C., Ancellet, G., Bechara, J., Borgon, A., Cairo, F., Coe, H., Gomes, L., Lambert, C., Law, K. S., Mari, C., Methven, J., Minikin, A., Nielsen, J. K., Schlager, H., and Thouret, V.: Chemical characterization of the troposphere over West Africa during the monsoon period as part of AMMA, in preparation, 2009. 19719, 19750

Ricaud, P., Barret, B., Attié, J.-L., Motte, E., Le Flochmoën, E., Teyssèdre, H., Peuch, V.-H., Livesey, N., Lambert, A., and Pommereau, J.-P.: Impact of land convection on troposphere-stratosphere exchange in the tropics, Atmos. Chem. Phys., 7, 5639–5657, 2007, http://www.atmos-chem-phys.net/7/5639/2007/. 19718

Ricaud, P., Pommereau, J.-P., Attié, J.-L., Le Flochmoën, E., El Amraoui, L., Teyssèdre, H., Peuch, V.-H., Feng, W., and Chipperfield, M. P.: Equatorial transport as diagnosed from nitrous oxide variability, Atmos. Chem. Phys. Discuss., 9, 4899–4930, 2009, http://www.atmos-chem-phys-discuss.net/9/4899/2009/.

Richard, E. C., Tuck, A. F., Aikin, C., Kelly, K. K., Herman, R. L., Troy, R. F., Hovde, S. J., Rosenlof, K. H., Thompson, T. L., and Ray, A.: High-resolution airborne profiles of CH_4, O_3, and water vapour near tropical Central America in late January to early February 2004, J. Geophys. Res., 111, D13304, doi:10:1029/2005JD006513, 2006.

Robinson, A. D., McIntyre, J., Harris, N. R. P., Pyle, J. A., Simmonds, P. G., and Danis, F.: A lightweight balloon-borne gas chromatograph for in-situ measurements of atmospheric halocarbons, Rev. Sci. Instrum., 71, 4553–4560, 2000. 19730

Rosen, J. M. and Kjome, N. T.: Backscattersonde – A new instrument for atmospheric aerosol research, Appl. Optics, 30, 1552–1561, 1991. 19733

Schiller, C., Krämer, M., Afchine, A., Spelten, N., and Sitnikov, N.: The ice water content of Arctic, mid latitude and tropical cirrus, J. Geophys. Res., 113, D24208, doi:10.1029/2008JD010342, 2008. 19717, 19725

Schiller, C., Grooß, J.-U., Konopka, P., Plöger, F., Silva dos Santos, F. H., and Spelten, N.: Hydration and dehydration at the tropical tropopause, in preparation, 2009. 19750, 19752

Sherwood, S. C. and Dessler, A. E.: Convective mixing near the tropical tropopause: Insights from seasonal variations, J. Atmos. Sci, 60, 2674–2685, 2003.

Shur, G. H., Sitnikov, N. M., and Drynkov, A. V.: A Mesoscale Structure of Meteorological Fields in the Tropopause Layer and in the Lower Stratosphere over the Southern Tropics (Brazil), Russ. Meteorol. Hydrol., 32, 487-494, 2007. 19729

Simões, F., Berthelier, J.-J., Godefroy, M., and Yahi, S.: Observation and modeling of the Earth-ionosphere cavity electromagnetic transverse resonance and variation of the D-region electron density near sunset, Geophys. Res. Lett., L14816, doi:10.1029/2009 GL039286, 2009.

Sitnikov, N., Yushkov, V., Afchine, A. A., Korshunov, L. I., Astakhov, V. I., Ulanovskii, A. E., Krämer, M., Mangold, M. A., Schiller, C., Ravegnani, F. : The FLASH instrument for water vapor measurements on board the high-altitude airplane, Russian Journal on Instruments and Experimental Techniques, 50(1), 113–121, 2007.

Slingo, A., Bharmal, N. A., Robinson, G. J., Settle, J. J., Allan, R. P., White, H. E., Lamb, P. J., Lele, M. I., Turner, D. D., McFarlane, S., Kassianov, E., Barnard, J., Flynn, C., and Miller, M.:

Overview of observations from the RADAGAST experiment in Niamey, Niger: Meteorology and thermodynamic variables, J. Geophys. Res., 113, D00E01, doi:10.1029/2008JD009909, 2008. 19723

Schmitt, J.: Construction and testing of an in-situ NO/NO_y measuring system aboard the high-altitude research aircraft M55-Geoophysica, PhD thesis, University Munich, DLR Research Report, ISRN-DLR-FB-2003-21, 2003. 19726

Spang, R., Hoffmann, L., Kullmann, A., Olschewski, F., Preusse, P., Knieling, P., Schroeder, S., Stroh, F., Weigel, K., and Riese, M.: High resolution limb observations of clouds by the CRISTA-NF experiment during the SCOUT-O_3 tropical aircraft campaign, Adv. Space Res., 42, 1765–1775, doi:10.1016/j.asr.2007.09.036, 2008. 19727

Sultan, B. and Janicot, S.: Abrupt shift of the ITCZ over West Africa and intraseasonal variability, Geophys. Res. Lett., 27, 3353–3356, 2000. 19721

Stefanutti, L., MacKenzie, A. R., Balestri, S., Khattatov, V., Fiocco, G., Kyrö, E., and Peter, T.: Airborne Polar Experiment-Polar Ozone, Leewaves, Chemistry, and Transport (APE-POLECAT): Rationale, road map and summary of measurements, J. Geophys. Res., 104(D19), 23941–23959, 1999. 19725

Suomi, V. E. and Kuhn, P. M.: An economical net radiometer, Tellus, 10, 160-163, 1958. 19731

Thomas, A., Borrmann, S., Kiemle, C., Cairo, F., Volk, C. M., Beuermann, J., Lepuchov, B., Santacesaria, V., Matthey, R., Rudakov, V., Yushkov, V., MacKenzie, A. R., and Stefanutti, L.: In-situ measurements of background aerosol and subvisible cirrus in the tropical tropopause region, J. Geophys. Res., 107(D24), doi:2001JD001385, 2002. 19729

Vernier, J. P., Pommereau, J. P., Garnier, A., Pelon, J., Larsen, N., Nielsen, J., Christensen, T., Cairo, F., Thomasson, L. W., Leblanc, T., and McDermid, I. S.: Troposphere stratosphere transport in the tropics from CALIOP lidar aerosols measurements, J. Geophys. Res., CALIPSO special issue, in press, 2009.

Viciani, S., D'Amato, F., Mazzinghi, P., Castagnoli, F., Toci, G., and Werle, P.: A cryogenically operated laser diode spectrometer for airborne measurement of stratospheric trace gases, Appl. Phys. B, 90, 581–592, 2008. 19726

Voigt, C., Schlager, H., Luo, B. P., Dörnbrack, A., Roiger, A., Stock, P., Curtius, J., Vössing, H., Borrmann, S., Davies, S., Konopka, P., Schiller, C., Shur, G., and Peter, T.: Nitric Acid Trihydrate (NAT) formation at low NAT supersaturation in Polar Stratospheric Clouds (PSCs), Atmos. Chem. Phys., 5, 1371–1380, 2005, http://www.atmos-chem-phys.net/5/1371/2005/. 19726

Voigt, C., Schlager, H., Roiger, A., Stenke, A., de Reus, M., Borrmann, S., Jensen, E., Schiller, C., Konopka, P., and Sitnikov, N.: Detection of reactive nitrogen containing particles in the tropopause region - evidence for a tropical nitric acid trihydrate (NAT) belt, Atmos. Chem. Phys., 8, 7421–7430, 2008, http://www.atmos-chem-phys.net/8/7421/2008/. 19753

Volk, C. M., Riediger, O., Strunk, M., Schmidt, U., Ravegnani, F., Ulanovsky, A., and Rudakov, V.: In situ Tracer Measurements in the Tropical Tropopause Region During APE-THESEO, Eur. Comm. Air Pollut. Res. Report 73, 661-664, 2000. 19726

von Hobe, M., Groo, J.-U., Müller, R., Hrechanyy, S., Winkler, U., and Stroh, F.: A re-evaluation of the ClO/Cl_2O_2 equilibrium constant based on stratospheric in-situ observations, Atmos. Chem. Phys., 5, 693–702, 2005, http://www.atmos-chem-phys.net/5/693/2005/. 19727

Weigel, R., Hermann, M., Curtius, J., Voigt, C., Walter, S., Böttger, T., and Borrmann, S.: Experimental characterization of the COndensation PArticle counting System for high altitude aircraft borne application, Atmospheric Measurement Techniques Discussions, 1, 321–374, 2008. 19728

Williams, E., Nathou, N., Hicks, E., Pontikis, C., Russell, B., Miller, M., and Bartholomew, M. J.: The Electrification of Dust-Lofting Gust Fronts ("Haboobs") in the Sahel, Atmos. Res., 91, 292–298, 2009. 19719

Yushkov, V., Merkulov, S., and Astakhov, V.: Optical balloon hygrometer for upper stratosphere and stratosphere water vapour measurements, in: Optical remote sensing of the atmosphere and clouds, edited by: Wang, J., Wu, B., Ogawa, T., and Guans, Z.-H., Proc. SPIE, 3501, 439–445, 1998. 19725, 19733

Yushkov, V., Oulanovsky, A., Lechenuk, N., Roudakov, I., Arshinov, K., Tikhonov, F., Stefanutti, L., Ravegnani, F., Bonafé, U., and Georgiadis, T.: A Chemiluminescent Analyzer for Stratospheric Measurements of the Ozone Concentration (FOZAN), J. Atmos. Ocean. Tech., 16, 1345-1350, 1999. 19726

Zipser, E. J., Cecil, D. J., Liu, C., Nesbitt, S. W., and Yorty, D. P.: Where are the most intense thunderstorms on Earth? B. Am. Meteorol. Soc., 1057–1071, 2006. 19717

Zöger, M., Afchine, A., Eicke, N., Gerhards, M. T., Klein, E., McKenna, D. S., Mörschel, U., Schmidt, U., Tan, V., Tuitjer, F., Woyke, T., and Schiller, C.: Fast in situ stratospheric hygrometers: A new family of balloonborne and airborne Lyman-a photofragment fluorescence hygrometers, J. Geophys. Res., 104, 1807–1816, 1999. 19725

Table 1. M55 flights, aims, instruments and data availability.

Date	31 July	1 August	4 August	7 August	8 August	11 August	13 August	16 August	17 August
Objective	UTLS profile	UTLS profile	UTLS profile	UTLS profile	MSC close-up	CALIOP val	MCS aged outflow	UTLS profile	UTLS profile
In situ tracers, H_2O									
FISH	ok	No data	ok	Ok	ok	Ok	ok	ok	ok
FLASH	Not present	Not present	ok	Ok	ok	Ok	No data	Not present	Not present
FOZAN	Not present	Not present	ok	ok	ok	Ok	ok	ok	ok
SIOUX	No data	No data	No data	ok	ok	No data	ok	ok	ok
HAGAR	ok	ok	ok	no data	ok	Ok	ok	ok	ok
ALTO	ok	No data	ok	ok	ok	No data	No data	ok	o
COLD	ok	Not present	No data	ok	ok	No data	Not present	Not present	Not present
IRIS	Not present	Not present	Not present	Ok*	Not present	Not present	Ok*	Ok*	Not present
HALOX	No data	No data	ok	ok	ok	Ok	ok	ok	ok
WAS	No data	No data	Ok*	ok	ok	Ok	ok	Not present	Not present
Remote Sensors									
MIPAS	ok	ok	ok	ok	ok	Ok	ok	ok	ok
CRISTA-NF	ok	ok	ok	ok	ok	Ok	ok	ok	Ok
Particles									(in situ)
COPAS_1	ok	ok	ok	Not present	ok	Ok	ok	ok	Ok
COPAS_2	ok	No data	ok	ok	ok	Ok	ok	ok	Not present
CIP	Not present	Not present	Not present	ok	ok	Ok	ok	ok	Ok
FSSP 100	ok	ok	ok	ok	ok	Ok	ok	ok	Ok
FSSP 300	No data	No data	Not present	Not present	Not present	Not present	Not present	Not present	Not present
MAS	ok	ok	ok	ok	ok	Ok	ok	ok	Ok
Meteorology									
UCSE	ok	ok	ok	ok	ok	Ok	ok	ok	ok
TDC	ok	Not present	ok	ok	ok	Ok	ok	ok	ok

ACPD
9, 19713–19781, 2009

Table 2. Balloon flights, aims, instruments and data availability.

Date	31 July	31 July	5 August	7 August	10 August	17 August	19 August	23 August
Objective	Aerosol	Ice and Aerosols 1	Water Vapour 1	Anvil and Cirrus 1	Chemistry 1	Ice and Aerosols 2	Chemistry 2	Water Vapour 2
In situ tracers, H_2O								
u-SDLA	Not present	Not present	Ok	Not present	Not present	Not present	Not present	Ok
u-Dirac	Not present	No data	No data	Not present	Ok (*)	Ok (*)	No data	Ok
Remote Sensors								
SAOZ	Not present	Not present	Not present	Ok	Ok	Not present	Ok	Not present
IR-rad	Not present	Not present	Not present	Ok	Not present	Not present	Not present	Not present
u-LIDAR	Not present	Not present	Not present	Ok	Not present	Not present	Not present	Not present
HV-AIRS	Not present	Not present	Not present	Ok	Not present	Not present	Not present	Not present
NILUcube	Not present	Not present	Not present	Not present	Ok	Not present	No data	Not present
Particles (in situ)								
OPC, CN, O_3	Ok	No data	Not present	Not present	Not present	Ok	Not present	Not present
LABS	Not present	Ok (*)	Ok	Not present	Not present	Ok	Not present	Ok
Meteorology								
Temperature, pressure	Ok	Ok	Ok	Ok	Ok	Ok	Ok	Ok

ACPD
9, 19713–19781, 2009

Table 3. Sonde flight dates and times, instruments and data availability.

Date, Time	Ozone	PTU	Backscattersonde	FLASH-B
26 July 2006 16:31	Ok	Ok	Not present	Not present
27 July 2006 15:13	Ok	Ok	Not present	Not present
28 July 2006 15:04	Ok	Ok	Not present	Not present
1 August 2006 13:49	Ok	Ok	Not present	Not present
2 August 2006 18:40	Ok	Ok	Ok	Not present
3 August 2006 10:00	Ok	Ok	Not present	Not present
3 August 2006 18:38	Ok	Ok	Ok	Ok
5 August 2006 09:26	Ok	Ok	Not present	Not present
5 August 2006 18:52	Ok	Ok	Ok	Ok
7 August 2006 10:34	Ok	Ok	Not present	Not present
7 August 2006 18:38	Ok	Ok	Ok	Ok
8 August 2006 09:32	Ok	Ok	Not present	Not present
9 August 2006 09:37	Ok	Ok	Not present	Not present
9 August 2006 18:39	Ok	Ok	Ok	Not present
10 August 2006 14:28	Ok	Ok	Not present	Not present
12 August 2006 08:59	Ok	Ok	Not present	Not present
12 August 2006 18:38	Ok	Ok	Ok	Not present
14 August 2006 09:11	Ok	Ok	Not present	Not present
14 August 2006 18:46	Ok	Ok	Ok	Ok
15 August 2006 10:22	Ok	Ok	Not present	Not present
16 August 2006 14:23	Ok	Ok	Not present	Not present
17 August 2006 09:43	Ok	Ok	Not present	Not present
18 August 2006 16:14	Ok	Ok	Not present	Not present
19 August 2006 15:27	Ok	Ok	Not present	Not present
21 August 2006 09:39	Ok	Ok	Not present	Not present
21 August 2006 21:52	Ok	Ok	Ok	Ok
23 August 2006 19:07	Ok	Ok	Ok	Ok
24 August 2006 09:13	Ok	Ok	Not present	Not present
25 August 2006 09:03	Ok	Ok	Not present	Not present

ACPD
9, 19713–19781, 2009

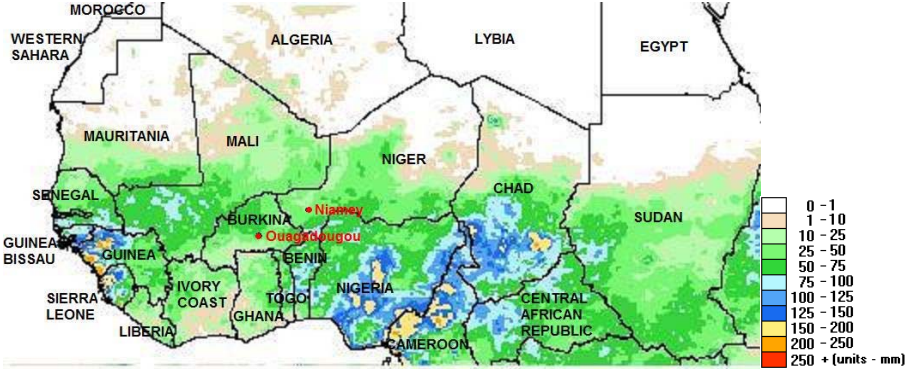

Fig. 1. Map of 1–10 August 2006 accumulated rainfall in West Africa (from the Goal of the Famine Early Warning Systems Network (FEWS NET) as a NOAA satellite imagery product (Tucker et al., 2005; Pinzon et al., 2004). Niamey and Ouagadougou are 400 km apart in the Sahel region.

ACPD
9, 19713–19781, 2009

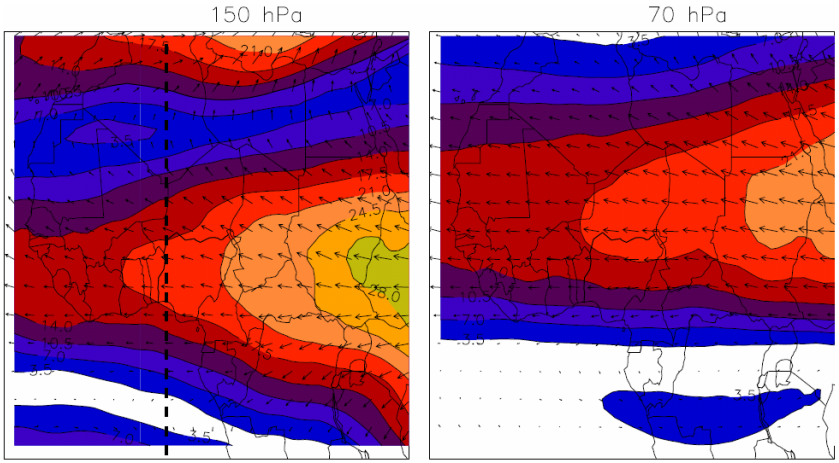

Fig. 2. Left panel, ECMWF reanalyzed wind module (m/s) and direction (vectors) for the 150 hPa level; the dashed line shows the 5° meridian, subsequently used for a vertical cross section (see Fig. 3). Right panel: as left but for the 70 hPa level. The average is done from 15 July to 16 August.

ACPD
9, 19713–19781, 2009

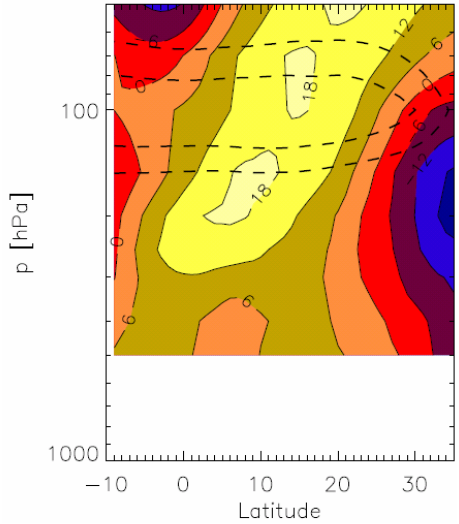

Fig. 3. ECMWF reanalyzed zonal wind cross section along the 5° meridian (as in the dashed line in Fig. 2). Temperature levels at −67 and −72°C are overlaid as dashed thick lines.

ACPD
9, 19713–19781, 2009

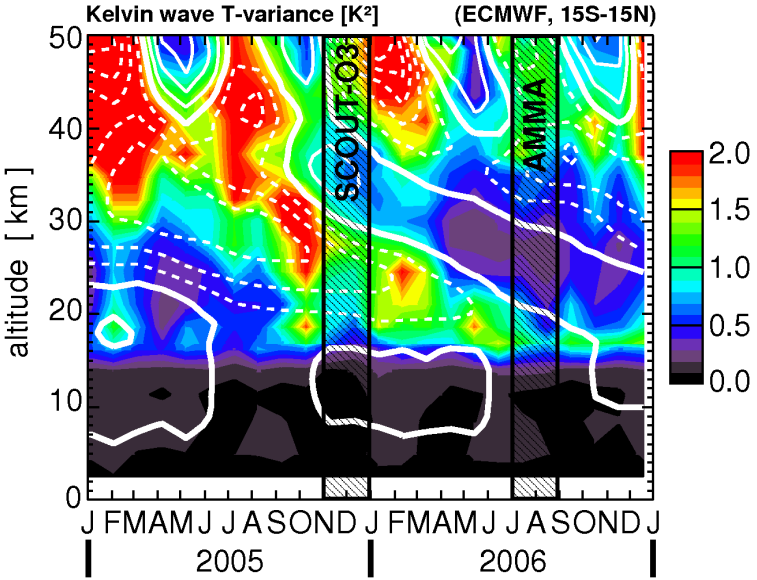

Fig. 4. Time series of 15° S–15° N average total Kelvin wave temperature variance derived from ECMWF operational analyses. Also shown are the 15° S–15° N average ECMWF zonal winds (white contours, contour increment is 10 m/s). The bold solid line is the zero wind line, solid contours are for westerlies, dashed contours for easterlies. Gray boxes evidence the time period for the Scout-O_3 Darwin and Scout-O_3 AMMA M55 campaigns.

ACPD
9, 19713–19781, 2009

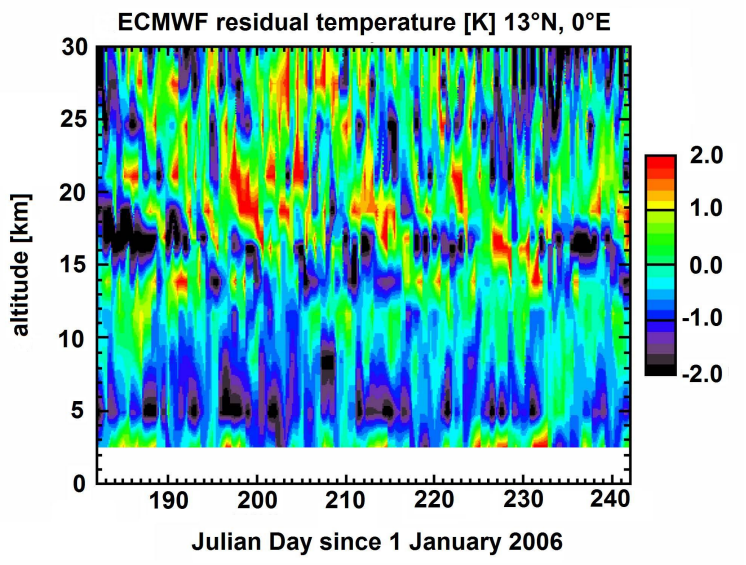

Fig. 5. ECMWF temperature anomaly (13° N, 0 E) for the period 1 July–30 August 2006.

ACPD
9, 19713–19781, 2009

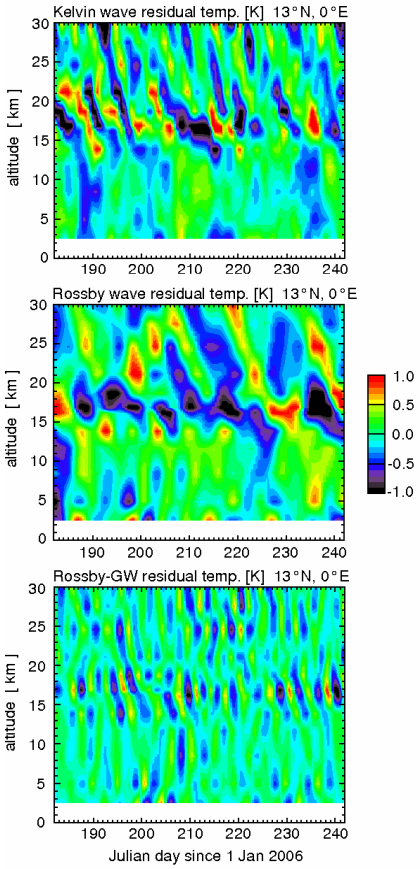

Fig. 6. Derived residual temperatures from a space-time spectral analysis for (13° N, 0 E) with band pass filters for the different equatorial wave modes applied. The results are shown for Kelvin (top panel), equatorial Rossby (middle panel) and Rossby-gravity waves (bottom panel).

ACPD
9, 19713–19781, 2009

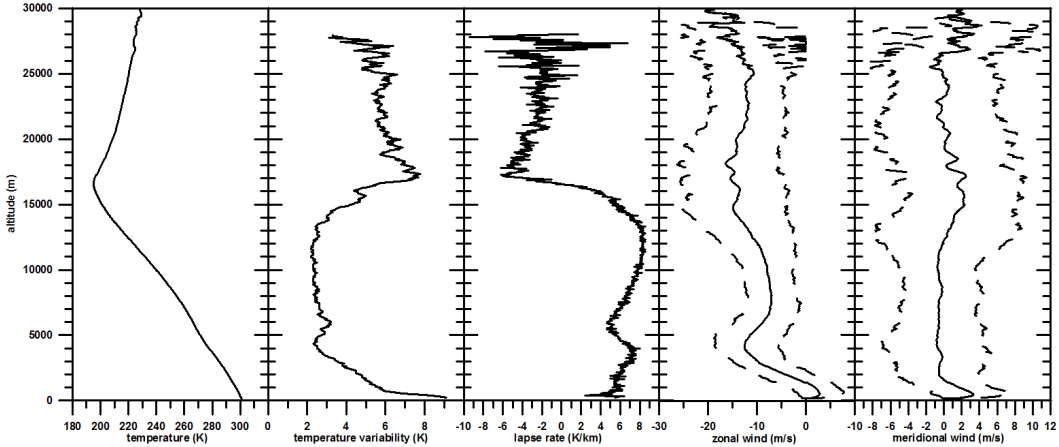

Fig. 7. From left to right: mean temperature, 10 to 90 percentiles temperature variability, lapse rate, zonal and meridional wind and 10- and 90-percentiles (red) from the 4 daily radiosoundings in Niamey.

ACPD
9, 19713–19781, 2009

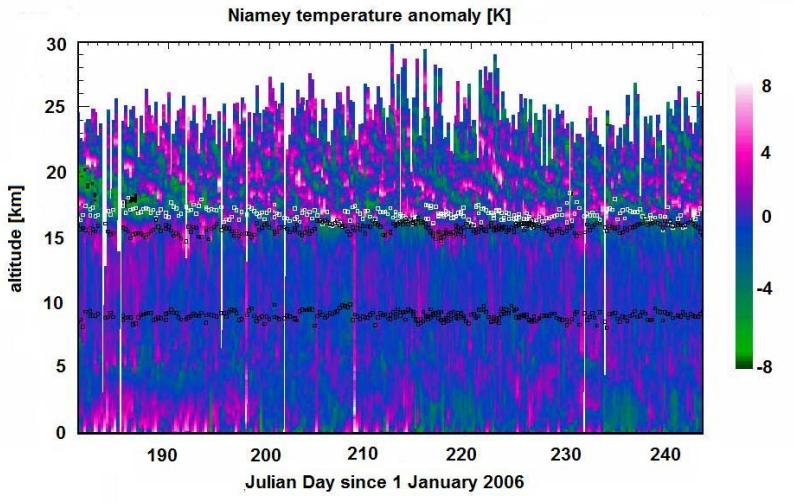

Fig. 8. Time series of temperature anomalies from the SOP2a2 radiosoundings in Niamey. White squares denote the altitude of the Cold Point Tropopause. The two black squared lines represent the 340 K and 365 K isentrope altitudes.

ACPD
9, 19713–19781, 2009

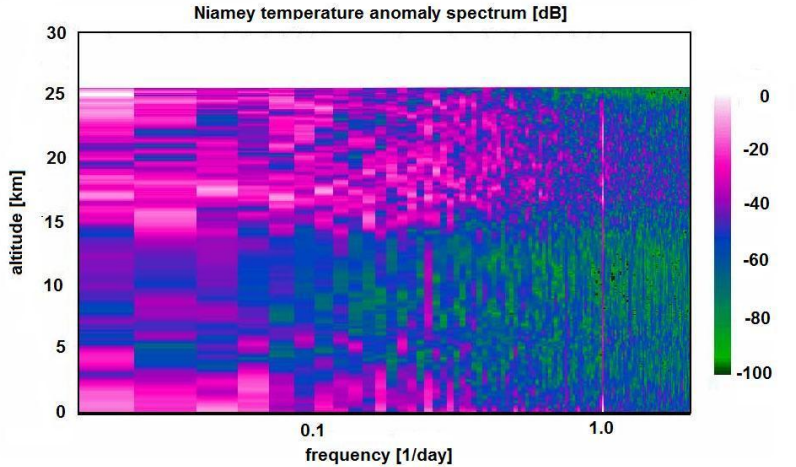

Fig. 9. Power spectrum of temperature anomaly time series.

ACPD
9, 19713–19781, 2009

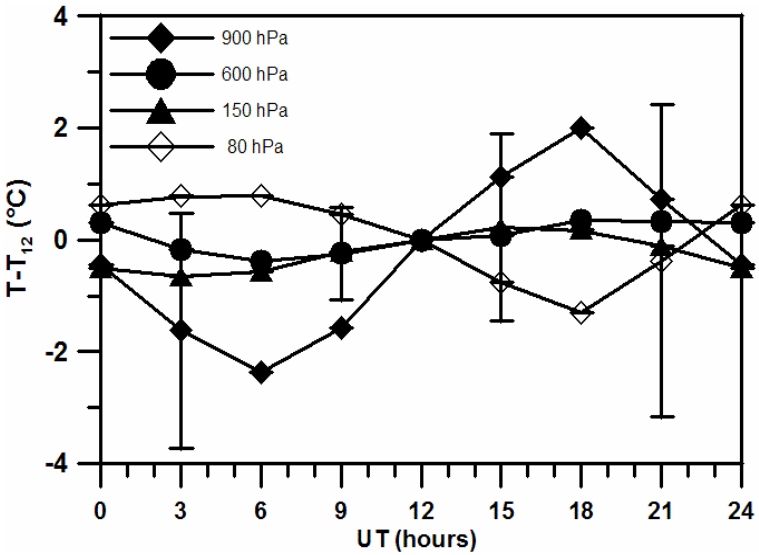

Fig. 10. Average diurnal temperature change at 900, 600, 150 and 80 hPa compared to noon-time from the 4 ARM soundings in Niamey from 1 July to 31 August reinforced to 8 soundings per day in 1–15 August.

ACPD
9, 19713–19781, 2009

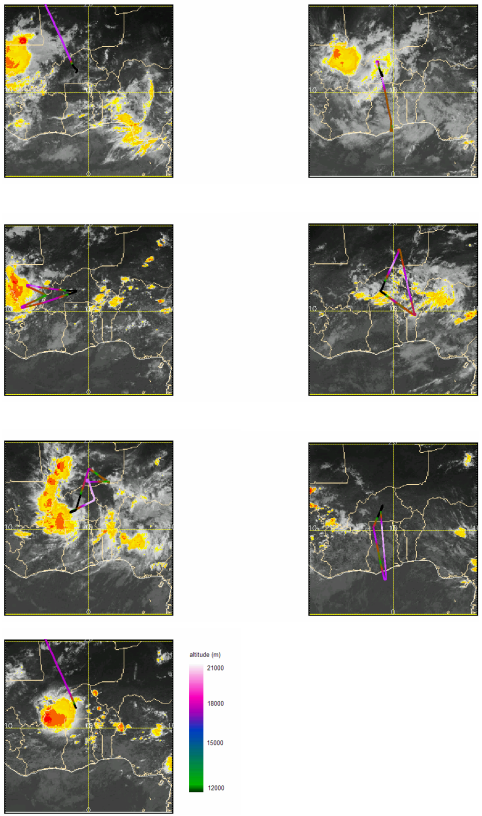

Fig. 11. M55 flight track superimposed to Meteosat IR 10.8 satellite images. Colours along the flight tracks codes the altitude. Images refer to the mid-time of the aricraft flight, panels from a to g are respectively from left to right and from top to bottom: 1 August at 13:00, 4 August at 10:00, 7 August at 14:00, 8 August at 13:30, 11 August at 16:30, 13 August at 14:30, 16 August at 15:00 (times are UTC). Colours on the image code the cloud brightness temperature, orange is colder than −65°C.

ACPD
9, 19713–19781, 2009

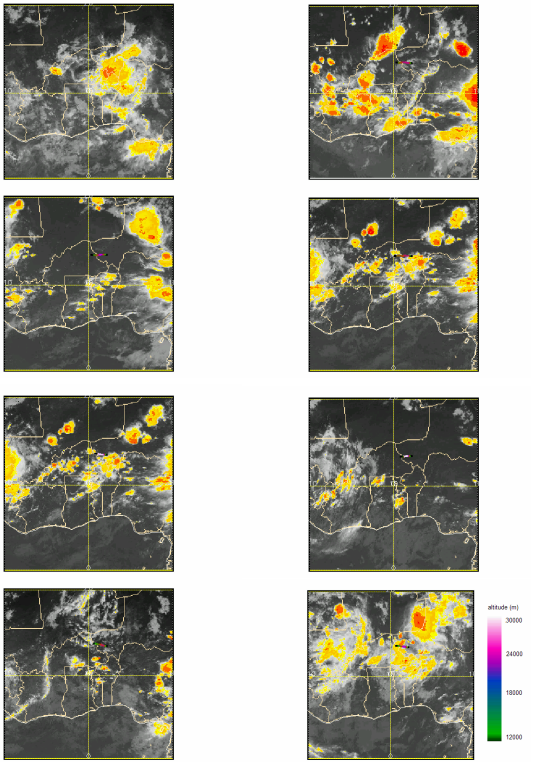

Fig. 12. Balloon flight track superimposed on MSG IR 10.8 um brightness temperature images. Images refer to the mid-time of the balloon flight, respectively from left to right and from top to bottom, 31 July at 10:00, 31 July at 19:30, 5 August at 20:30, 7 August at 18:30, 10 August at 18:00, 17 August at 13:30, 19 August at 18:00, 23 August at 20:00 (times are expressed in UTC). Colours along the flight tracks codes the altitude. Colours on the image code the cloud brightness temperature, orange is colder than −65°C. On the first figure, the balloon flight track is not present due to lack of geolocation of the flight payload.

ACPD

9, 19713–19781, 2009

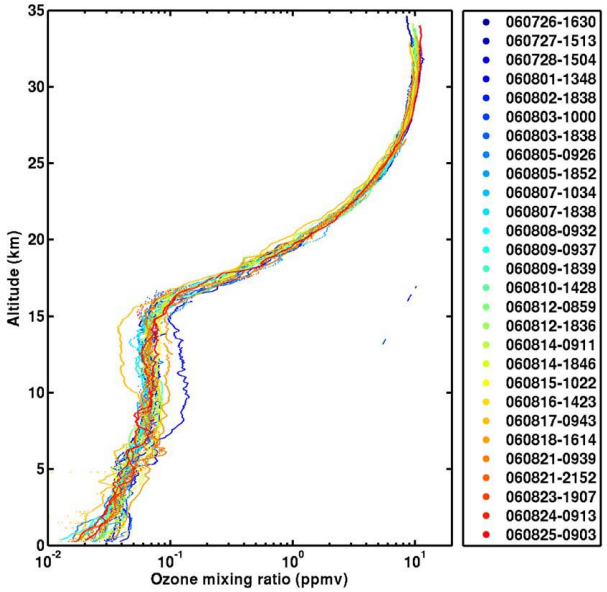

Fig. 13. Vertical profiles of ozone mixing ratio from 28 ozone soundings from Niamey between 26 July and 25 August 2006.

ACPD
9, 19713–19781, 2009